

A new dynamic model of crude oil fouling deposits and its application to the simulation of fouling-cleaning cycles

E. Diaz-Bejarano¹, F. Coletti², and S. Macchietto^{1,2*}

¹Department of Chemical Engineering, Imperial College London, London SW7 2AZ, UK

²Hexxcell Ltd., Imperial College Incubator, Bessemer Building Level 2, Imperial College London, London SW7 2AZ, UK,

Corresponding author: s.macchietto@imperial.ac.uk

Modelling of crude oil fouling in heat exchangers has been traditionally limited to a description of the deposit as a thermal resistance. However, consideration of the local change in thickness and the evolution of the properties of the deposit due to ageing or changes in foulant composition is important to capture the thermal and hydraulic impact of fouling. A dynamic, distributed, first-principles model of the deposit is presented that considers it as a multi-component varying-thickness solid undergoing multiple reactions. For the first time, full cleaning, partial cleaning and fouling resumption after cleaning can be simulated in any order with a single deposit model. The new model, implemented within a single tube framework, is demonstrated in a case study where various cleaning actions are applied following a period of organic deposition. It is shown that complete mechanical cleaning and chemical cleaning of different extent, according to a condition-based efficacy, can be seamlessly simulated.

Keywords: crude oil, fouling, mathematical model, cleaning, simulation,.

Introduction

The preheat train (PHT) of crude distillation units is a key facility for the energy efficiency of refineries.

The deposition of unwanted material from crude oil on heat transfer surfaces of PHT heat exchangers has a dramatic effect on heat recovery, leading to substantial energy losses, fuel consumption, operating

This article has been accepted for publication and undergone full peer review but has not been through the copyediting, typesetting, pagination and proofreading process which may lead to differences between this version and the Version of Record. Please cite this article as doi: 10.1002/aic.15036

© 2015 American Institute of Chemical Engineers (AIChE)

Received: May 16, 2015; Revised: Aug 17, 2015; Accepted: Sep 08, 2015

This article is protected by copyright. All rights reserved.

difficulties and CO₂ emissions¹. The hot end of the PHT is typically the section more severely affected by fouling. Studies suggest that mitigation of fouling in these facilities could lead to significant fuel and energy savings². As a result, research has traditionally focused on this section³, with fouling from organic materials as the main mechanism.

Traditional heat exchanger design and monitoring methodologies rely on fixed fouling factors to describe the additional resistance to heat transfer generated by the presence of fouling (i.e. fouling resistance, R_f). However, fouling is an intrinsically dynamic process which leads to a gradual degradation of the thermal performance of heat exchangers. The study of the dynamics of crude oil fouling, i.e. fouling rate, has traditionally focused on the development of expressions to capture the change in thermal resistance over time. The most widely used models to quantify crude oil fouling in refineries are the semi-empirical “threshold” models, such as the one originally proposed by Ebert and Panchal⁴. These models are based on the approach first introduced by Kern and Seaton⁵, which represents fouling rate as the difference between two processes, deposition and suppression (or removal, depending on the author). Threshold models represent a pragmatic approach to capture the influence of the main variables affecting crude oil fouling (flow velocity and temperature^{2,6,7}) and provide a useful tool to study the basic effects of fouling on design and operations⁸. More rigorous mechanistic models have been proposed considering kinetics⁶ and mass transfer⁹ as the limiting steps, but the complexity of the process makes a complete mechanistic description of the fouling process a still unresolved challenging problem. An aggregate, average fouling resistance is typically used (i.e. a single value for a whole heat exchanger). On the other hand, it is well known that different deposition occurs in various parts of a heat exchanger, and capturing the (local) resistance accurately is clearly important.

The local resistance to heat transfer offered by the deposit depends not only on the (local) fouling rate, but also on the (local) evolution of the physical properties of the deposit (in particular, its thermal conductivity). This is neglected in the previously cited fouling models, as are pressure effects. The deposit layer is the actual entity that represents the entire difference between a fouled and clean exchanger and its thermal and hydraulic performance (and, in fact, is the nexus between those two). As a result, it is important to differentiate between: i) modelling of the fouling rate (addition or removal of material to the existing layer) and ii) modelling of the deposit itself. Table 1 shows the evolution over the past 10 years of models

used to describe crude oil fouling deposits in shell-and-tube PHT heat exchangers. Gradual additions to traditional R_f -based methodologies include representation of: i) deposit thickness; ii) ageing of the organic material; iii) spatial distribution; iv) deposit composition and reactions (including ageing).

Fouling has a significant hydraulic effect since it gradually reduces a tube cross sectional area, restricting flow and increasing pressure drop, and can even lead to complete blocking of the tubes. The reduction in flow area also leads to increase of shear forces which, in turn, reduce the net deposition rate. Therefore, it is important to consider this aspect in crude oil fouling modelling. One way to capture the hydraulic impact of fouling (pressure drop) is by relating the overall R_f to an average thickness of the layer (δ_l) through an average thermal conductivity (λ_l) according to the thin-slab approximation ($R_f \approx \delta_l/\lambda_l$). By coupling this expression with a thermal fouling model, the average growth of the layer can be estimated^{3,10}. This assumption, however, is only valid if the thickness of the layer is less than about 10% of the inner diameter of the tube, which is vastly exceeded in common practice in PHT tubes. It also requires having a correct thermal conductivity, which is neither constant, nor uniform across and along a tube.

Significant progress in the description of crude oil fouling deposit was achieved by including ageing. Ageing of crude oil organic fouling deposits is defined as the gradual degradation of ‘fresh’ organic deposit into coke at high temperature¹¹. These changes in the micro-structure of the deposit affect the physical properties of the layer^{12,13}: thermal conductivity, which increases over time affecting heat transfer; and mechanical properties, with gradual hardening of the deposit making it more difficult to remove. In order to account for ageing, Crittenden and Kolaczowski¹⁴ included a term in the expression for fouling rate to account for the reduction in fouling resistance as a result of coking of the organic layer, based on pioneering work for coking in crude oil furnaces¹⁵⁻¹⁷. This work still views the deposit layer as a single thermal resistance. More recently, Ishiyama et al.¹² proposed an Arrhenius-type kinetic model for ageing of fouling deposits. The model describes ageing as the evolution from the low conductivity of fresh organic deposit (“gel”, $\lambda_l \approx 0.1-0.2$ W/mK), to the enhanced conductivity of “coke” ($\lambda_l \approx 1$ W/mK) as a function of temperature. The ageing kinetics is expressed in terms of a “youth” variable that varies from 1 (fresh deposit) to 0 (completely aged deposit). This kinetic model was combined with a (still lumped for an entire exchanger) deposit model that consists of multiple thermal resistances in series that start ageing at fixed time intervals, each according to a first order kinetics scheme. Later work¹⁸ tested alternative formulations, such

as zero order kinetics, and simplified versions of the deposit model, such as a double fouling resistance model (gel-coke). The multi-layer and the simplified two-layer model were compared for fouling build-up at various ageing rates. Due to disagreement in the calculated fouling resistance under some operating conditions, the paper's authors recommended caution when using a double-layer approach to extract model parameters, confirm ageing effects and predict fouling impact under conditions different to those used in the estimation. The kinetic ageing model was refined by Coletti et al.¹³ within a more rigorous dynamic, continuous and (axially and radially) distributed model, overcoming the many assumptions in the above fixed, multi-layer approach. These studies, which capture ageing as a change in layer conductivity, highlighted its potential impact over long operation periods and the importance of coupling this effect with appropriate deposition models for correct interpretation of experimental and operational data¹³. Due to a lack of available measurements, it has not been possible to formally validate this kinetic ageing model^{12,13} against experimental data.

Coletti et al.¹³ replaced the simplified lumped thermal description of the layer as R_f with a first principle dynamic and distributed heat balance. It includes a moving boundary formulation to capture the growth of the deposit, which, at the same time, eliminates the need of the thin-slab assumption. The model was implemented within a dynamic, distributed shell-and-tube heat exchanger software where various single and multi-pass configurations are easily defined, was tested against plant data showing excellent prediction capabilities² and is now available commercially¹⁹. A number of instances of the heat exchanger model can be linked to simulate entire sections of a preheat train and study the effects of fouling network-wide^{20,21}. This work showed the importance to the overall thermal performance of a heat exchanger of capturing the full local thermal conductivity profiles as a function of the distinct temperature history of each point in a deposit layer, and in particular the increase in thermal conductivity over time due to ageing. However, the model still presents some limitations, such as the inability to simulate partial removal and subsequent re-deposition on an old layer. This is relevant, for instance, when trying to describe various deposition-limiting mechanisms and partial cleaning activities.

A modified version of the previous model² was recently developed by Diaz-Bejarano et al.²² for inorganic as well as organic deposits and shown to explain plant data in a field study of the Esfahan Refinery (Iran)²³. A weighted average of the conductivity between the inorganic and the organic portion was

proposed. This formulation limits its applicability to deposits with two pseudo-components (not genuine multi-component) in fixed proportions, and is still not able to cope with concentration changes over time. However, this work showed the need to consider the effect of composition (other than gel-coke) on the thermal properties of deposits and its important role in explaining both thermal and hydraulic performance of a heat exchanger.

Using an altogether different approach, advanced simulation techniques, such as computational fluid dynamics (CFD)^{24–29} or direct numerical simulation (DNS)²⁴, have been proposed to develop highly detailed mechanistic deposition models including effect of oil composition and phenomena such as diffusion, adhesion, chemical reaction and sophisticated rheology. For instance, in reference²⁵ the deposit is conceived as a distinct fluid phase with high viscosity, rather than as a solid, interacting with a bulk crude oil liquid phase. The ageing process affects its conductivity and rheology, making it more conductive and viscous over time. These models are still under development, are limited by a lack of fundamental understanding to the level of detail demanded, and in most cases are unable to simulate industrially relevant equipment and time scales.

Despite mitigation actions fouling eventually builds up and periodic cleaning is required to restore the performance of heat exchangers³⁰. Cleaning is usually carried out either mechanically with high pressure water jet or by circulating chemicals through the heat exchanger⁷. A mechanical cleaning requires taking the heat exchanger off-line for up to a week and typically results in a complete removal of deposits. Chemical methods have a smaller impact on operations (i.e. it can be done in situ, in some cases without requiring to dismantle the unit) thus have a quicker turnaround time. The efficacy of the treatment depends on a number of factors (e.g. choice of chemicals with respect to deposits' composition³¹) and in many cases not all the deposit is removed from the tube surfaces.

The use of optimization to assist in the complicated task of scheduling cleaning activities in PHTs (which units to clean and when) has attracted the attention of many researchers over the past years³². The decision is ultimately based on an economic trade-off between (mainly) the energy losses due to fouling, the cost of cleaning and loss of production, and on the other hand increased throughput and energy recovery after a cleaning. Models normally used in these studies treat the fouling deposit as a simplified thermal resistance (at best) and ignore any changes in the physical properties over time. Cleaning is generally

assumed to completely restore the heat exchangers to the original performance (total cleaning) and cleaning times are fixed. In reality, the effectiveness of the cleaning depends on the cleaning method and on the properties of the fouling layer produced thus far. Ishiyama et al.³³ used their simple double-layer deposit model and considered two types of cleaning: i) total cleaning, associated to mechanical methods and assumed to completely restore performance; and ii) partial cleaning, associated to chemical methods and assumed to remove only the gel layer. The partial cleaning time is fixed and independent of the coking state of the deposit. Due to its simplicity, this model could be used to optimize cleaning schedules^{33–35}. Albeit in a simplified way, this is the first attempt to include both types of cleaning.

The goal of this work is to tackle all the above issues in a comprehensive, unified way, overcoming current limitations and expanding the range of model applicability to include fouling, cleaning (partial and total) and resumption of fouling from a partially cleaned surface, all within the same model. First, a deposit layer model is presented that extends and generalises the work by Coletti & Macchietto² and Diaz-Bejarano et al.²². The new model describes the deposit as a multi-component system undergoing multiple reactions (such as ageing) in a varying-thickness solid layer. Appropriate formulation of boundary conditions and solution method are presented allowing for the seamless transition between operating modes. In the section *Deposition, ageing and cleaning models*, some classical deposition and ageing models are recast in this reaction engineering framework. In addition, models for chemical and mechanical cleaning methods are proposed. The new deposit model, implemented within a previously developed software framework for a single tube, is then demonstrated in the section *Application: Fouling-Cleaning Cycle* through a case study where full and various types of condition-dependent partial cleaning actions are applied, following and followed by periods of organic deposition. The implications of the new approach and future prospects are discussed in the last section.

Multi-component model of fouling layer undergoing chemical reactions

The system considered is a single tube with crude oil flowing inside the tube, depicted in Figure 1. Consistently with previous work², it is modelled in cylindrical coordinates with distributions in both the radial domain (r) and the axial domain (z) including three domains: tube-side flow domain ($\Omega_t \forall r < R$ –

$\delta_l(t)$, tube wall ($\Omega_w \forall r \in [RI, RO]$), and fouling deposit domain ($\Omega_l \forall r \in [RI - \delta_l(t), RI]$), where RO and RI are the outer and inner tube radius, respectively, and $\delta_l(t)$ is defined below.

The equations for the tube-side flow and tube wall domains (including boundary initial conditions and solution scheme) were reported in previous work¹³ and are not repeated here. However, a new model for the fouling deposit layer is defined in the following. As indicated, the fouling layer domain is denoted by (Ω_l), where subscript l stands for layer. At each coordinate z , the radial domain is defined for r between the inner tube wall radius (RI) and the surface of the fouling layer of thickness (δ_l), located at ($R_{flow}(z) = RI - \delta_l(t, z)$). The layer thickness varies with time due to deposition (e.g. during normal operation) or removal (e.g. during cleaning). It is assumed that the layer behaves as a solid and that oil and deposit are homogeneous in the angular direction.

As in previous work¹³, assuming negligible heat transfer in the axial direction and negligible heat of reaction, the temperature at each point in the deposit layer is defined by the conductive heat balance equation:

$$\rho_l(z, r) C_{p,l}(z, r) \frac{\partial T_l(z, r)}{\partial t} = \frac{1}{r} \frac{\partial}{\partial r} \left(r \lambda_l(z, r) \frac{\partial T_l(z, r)}{\partial r} \right) \quad (1)$$

where T_l is temperature, ρ_l density, $C_{p,l}$ specific heat capacity, and λ_l thermal conductivity at each point (z, r).

The boundary condition for the layer at RI is:

$$q_w''|_{r=RI} = q_l''|_{r=RI} \quad (2)$$

$$T_w|_{r=RI} = T_l|_{r=RI} \quad (3)$$

At the surface, R_{flow} (moving boundary):

$$q_l''|_{R_{flow}} = -h(T_l|_{R_{flow}} - T_t) \quad (4)$$

where q'' is the heat flux, h the heat transfer coefficient, and T_t the bulk oil temperature.

Unlike previous work¹³, it is assumed each point of the layer is also characterised by the mass concentration $c_{l,i}(z, r)$ and volume fraction $x_{l,i}(z, r)$ of a number $i = 1, \dots, NC$ of components (e.g., gel, coke, inorganic salt 1, inorganic salt 2, etc.). Mass concentration and volume fraction of each species i are linked via their density as follows.

$$c_{l,i}(z, r) = \rho_l x_{l,i}(z, r) \quad (5)$$

Furthermore, it is assumed that at each point the components in the layer may undergo a number NR of reactions between them (e.g. conversion of gel to coke), where r_j is the reaction rate of reaction j ($j = 1 \dots NR$) and ν_{ij} is the stoichiometric coefficient of component i in reaction j . The mass conservation law for the i^{th} component in cylindrical coordinates is:

$$\frac{\partial c_{l,i}(z, r)}{\partial t} = \frac{1}{r} \frac{\partial}{\partial r} \left(r D_i(z, r) \frac{\partial c_{l,i}(z, r)}{\partial r} \right) + \sum_{j=1}^{NR} \nu_{ij} r_j(z, r) \quad (6)$$

where D_i is the diffusion coefficient of component i in the mixture. Diffusion might be important in some cases³⁶, and if so Eq. 6 should be used. If diffusion through the solid layer is negligible and the concentration at a given point r is assumed to only change due to chemical reaction, Eq. (6) can be simplified to:

$$\frac{\partial c_{l,i}(z, r)}{\partial t} = \sum_{j=1}^{NR} \nu_{ij} r_j(z, r) \quad (7)$$

The deposit has been assumed to be non-porous. Further modification could be also considered to include this feature.

At each point (z, r) the physical properties of the layer ($\rho_l, C_{p,l}, \lambda_l$) depend on the local composition. Density and heat capacity are defined as the mass weighted average of those of the components (Eqs. 8, 9). The effective conductivity of heterogeneous materials depends on the number of phases, internal structure, degree of mixing and porosity. A number of models considering various structures can be found in literature³⁷. Unless such information is available, the local effective conductivity at each point (z, r) is calculated as the volumetric weighted average of the conductivities of the individual components (λ_i) (Eq. 10).

$$\rho_l(z, r) = \sum_{i=1}^{NC} c_{l,i}(z, r) \quad (8)$$

$$C_{p,l}(z, r) = \frac{1}{\rho_l(z, r)} \sum_{i=1}^{NC} c_{l,i}(z, r) C_{p,i} \quad (9)$$

$$\lambda_l(z, r) = \sum_{i=1}^{NC} x_{l,i}(z, r) \lambda_i \quad (10)$$

Lagrangian Transformation: Variable grid

In order to more easily solve an equation system with a moving boundary condition, a Lagrangian transformation of the coordinate system is proposed, moving from a fixed grid (with a moving boundary) to a variable grid (with fixed and normalized boundaries). A schematic representation of this change in coordinates is shown in Figure 2, which shows the layer on the left at time t_1 and on the right at a later time t_2 when it has grown deeper. The composition along the radial dimension may vary over time due to chemical reactions, in particular closer to the tube wall. This is represented as a gradual darkening in the figure. In dimensional coordinates (top part of Figure 2) a differential element of fouling material located at a distance $(RI - r)$ from the wall has a composition which is only affected by the chemical reactions. In dimensionless coordinates (bottom part of Figure 2), however, the element both “moves” through the dimensionless domain to account for the growth (or reduction) of the layer thickness and, simultaneously, undergoes chemical reaction as in the dimensional case.

In general terms, a variable F can be expressed in two coordinate systems using alternative formulas:

$$F(t, r) = \bar{F}(\tilde{t}(t), \tilde{r}(t)) \quad (11)$$

By applying the multivariate chain rule:

$$\frac{dF(t, r)}{dt} = \frac{\partial \bar{F}(t, \tilde{r}(t))}{\partial t} + \frac{\partial \bar{F}(t, \tilde{r}(t))}{\partial \tilde{r}} \frac{d\tilde{r}(t)}{dt} \quad (12)$$

The partial derivative with respect to r is:

$$\frac{\partial}{\partial r} = \frac{\partial}{\partial \tilde{r}} \frac{\partial \tilde{r}}{\partial r} \quad (13)$$

In the specific case of the solid layer, the interval $[RI, RI - \delta_l(t)]$ is re-scaled by introducing a dimensionless variable:

$$\tilde{r}_l(t) = \frac{RI - r}{\delta_l(t)} \quad (14)$$

\tilde{r}_l is defined for the closed interval $[0,1]$: at $r=RI$, $\tilde{r}_l = 0$; and at $r=RI - \delta_l(t)$, $\tilde{r}_l = 1$. By applying the above transformation to equations (1) and (7) yields:

$$\rho_l(z, \tilde{r}_l) C_{p,l}(z, \tilde{r}_l) \left(\frac{\partial T_l(z, \tilde{r}_l)}{\partial t} - \frac{\tilde{r}_l}{\delta_l(z)} \dot{\delta}_l(z) \frac{\partial T_l(z, \tilde{r}_l)}{\partial \tilde{r}_l} \right) = \quad (15)$$

$$\frac{1}{(RI - \tilde{r}_l \delta_l(z)) \delta_l(z)^2} \frac{\partial}{\partial \tilde{r}_l} \left((RI - \tilde{r}_l \delta_l(z)) \lambda_l(z, \tilde{r}_l) \frac{\partial T_l(z, \tilde{r}_l)}{\partial \tilde{r}_l} \right) - \left(\frac{\partial c_{l,i}(z, \tilde{r}_l)}{\partial t} - \frac{\tilde{r}_l}{\delta_l(z)} \delta_l(z) \frac{\partial c_{l,i}(z, \tilde{r}_l)}{\partial \tilde{r}_l} \right) = \sum_{j=1}^{NR} v_{ij} r_j(z, \tilde{r}_l) \quad (16)$$

where δ_l , the rate of change in thickness of the fouling layer δ_l , is actually a volumetric flux of material (net flux):

$$\delta_l = \frac{d\delta_l}{dt} \left[\frac{m^3}{m^2 s} \right] = \left[\frac{m}{s} \right] \quad (17)$$

The second term on the left hand side of Eqs. (15-16) enables conveying information through the radial dimensionless domain as the layer thickness changes. This formulation links the heat and mass balances to the variation of the thickness of the layer and also relates the inside of the layer to the processes (deposition, removal or reactions) occurring at the boundary. As a result, it is possible to represent, if so wished, the independent deposition of individual components (e.g. salts or asphaltenes) on the top layer, changes in fouling behaviour (e.g. further to an oil blend change or operations malfunction), and local composition-temperature based changes within the deposit layer. Any assumptions on the age of the different sub-layers of the deposit¹³ become unnecessary, and the entire previous history at each point (e.g. of concentration, temperature) is reflected by the state variables describing it.

This kind of transformation was used elsewhere for the single-component mass balance applied to growth of wax deposits undergoing ageing, modelled as a gradual change in porosity by diffusion^{36,38,39}. Here, it is applied both to a general multi-component mass balance and to the dynamic heat balance for the deposit layer. It is highlighted that this model is not only valid for layer growth, but also permits describing a thickness reduction without loss of composition information. The variation of the deposit thickness is given by the net combination of fouling deposition rate and any other mechanisms that promote deposition or removal, such as cleaning.

Boundary Condition for Deposit Mass Balance

The concentration at the surface is determined by the net effect of the deposition and removal processes taking place at each time and location. When the deposit grows, a particle just deposited is immediately

covered by new deposit. The net effect is that fresh deposit is seen at the boundary. When the deposit is reduced, as the top layer is removed, it uncovers the immediately underlying material; the net effect is that fresh deposit is not seen at the boundary.

The boundary conditions are evaluated locally for each z along the tube, although this is not shown explicitly in the following. $c_{l,i}(t,1^+)$ is defined as the concentration of component i just inside the layer boundary, $c_{l,i}(t,1^-)$ as its concentration just outside of the layer, and ζ as the distance between those two points. In general, the mass balance for component i at the boundary of the dimensionless domain is:

$$\left[2\pi\tilde{r}_l\xi\Delta z \left(\frac{\partial c_{l,i}}{\partial t} \right) \right]_{\tilde{r}_l=1^+} = \left[2\pi\tilde{r}_l\Delta z c_{l,i}\delta_L \right]_{\tilde{r}_l=1^-} - \left[2\pi\tilde{r}_l\Delta z c_{l,i}\delta_L \right]_{\tilde{r}_l=1^+} + \left[2\pi\tilde{r}_l\xi\Delta z \sum_{j=1}^{NR} v_{ij}r_j \right]_{\tilde{r}_l=1^+} \quad (18)$$

Two cases are distinguished. First, if the rate of change in thickness is substantially different from zero at the boundary, then $\zeta/\delta_L \rightarrow 0$ (where ζ is a small number) and:

$$[c_{l,i}]_{\tilde{r}_l=1^-} = [c_{l,i}]_{\tilde{r}_l=1^+} \quad (19)$$

The final formulation of this boundary condition depends on the rate of change in deposit thickness:

- a) If the thickness increases over time ($\delta_L > 0$), i.e. fouling builds up, the concentration of each species i at the deposit boundary is the concentration of the fresh material being deposited, $c_{fresh,i}$. As a result, Eq. (19) becomes:

$$c_{l,i}|_{\tilde{r}_l=1} = c_{fresh,i}(t) \quad (20)$$

The concentration of the fresh material is determined by the net deposition of the different fouling species:

$$c_{fresh,i} = \frac{n_{f,i}}{\sum_i^N n_{f,i}/\rho_i} \quad (21)$$

where $n_{f,i}$ is the net deposition rate of species i (a mass flux, with units [kg/m²s]).

- b) If there is a net flux of material leaving the fouling layer and its thickness decreases over time (i.e. $\delta_L < 0$), the value of $c_{l,i}(t,1^-)$ is the composition of the material leaving the layer. Eq. (19) becomes:

$$\left. \frac{\partial c_{l,i}(t)}{\partial \tilde{r}_l} \right|_{\tilde{r}_l=1} = 0 \quad (22)$$

Second, if the rate of change in thickness is negligible, i.e. $\dot{\delta}_l/\xi \rightarrow 0$, Eq. (18) becomes:

$$\left[\frac{\partial c_{l,i}}{\partial t} \right]_{\tilde{r}_l=1} = \left[\sum_{j=1}^{NR} v_{ij} r_j \right]_{\tilde{r}_l=1} \quad (23)$$

Therefore, the mass balance (Eq. 7) applies at the boundary. This assumes that the surface of the layer is unaffected by shear forces and deposition. Other scenarios could apply, such as balanced deposition and removal.

All three situations given by Eq. (20, 22, 23) may be encountered at different times. In practice, the transition between boundary conditions could be difficult to solve numerically. Alternatively, by combining the above boundary conditions equations, a single set of equations that describe all cases can be devised:

$$\left[\xi \frac{\partial c_{l,i}}{\partial t} \right]_{\tilde{r}_l=1} = (c_{fresh,i} - c_{l,i}|_{\tilde{r}_l=1}) \dot{\delta}_l + \left[\xi \sum_{j=1}^{NR} v_{ij} r_j \right]_{\tilde{r}_l=1} \quad \forall \dot{\delta}_l \geq 0 \quad (24)$$

$$\frac{\partial c_{l,i}}{\partial t} \Big|_{\tilde{r}_l=1} = \left[\frac{1}{\delta_l} \dot{\delta}_l \frac{\partial c_{l,i}}{\partial \tilde{r}_l} \right]_{\tilde{r}_l=1} + \left[\sum_{j=1}^{NR} v_{ij} r_j \right]_{\tilde{r}_l=1} \quad \forall \dot{\delta}_l < 0 \quad (25)$$

When the rate of change in thickness is significant ($\dot{\delta}_l \gg 0$ or $\dot{\delta}_l \ll 0$), the terms multiplied by ξ are negligible and equations (24) and (25) become Eq. (20) and (22), respectively. Conversely, if $\dot{\delta}_l \rightarrow 0$, the term multiplied by $\dot{\delta}_l$ is negligible and the top layer behaves just as the rest of the deposit. In that case, the boundary condition becomes Eq. (23). As a result, the proposed boundary conditions (Eq. 24, 25) enable a numerically smooth transition between net deposition, removal and the case in which the deposit thickness barely changes. A secondary consequence of this formulation is the ability to simulate abrupt changes of composition at the boundary, which might happen when deposition re-starts following removal, the type of foulant or (or anti-foulant) changes, etc. The value of ξ , the discretization and the numerical solution scheme must be fine-tuned so as to give stable numerical results and, at the same time, permit a smooth transition between the various cases. Further details are given in Appendix I.

This new model for the deposit layer domain was implemented within the overall model for a heat exchanger tube developed in previous work (i.e. with the same tube wall and tube-side flow equations), however with the new layer domain equations and boundary conditions described in this section.

Two operation modes for the tube were considered: uniform heat flux (UHF) and uniform wall temperature (UWT). Alternatively, a tube bundle could be considered, with the boundary condition at the outer surface of the wall connected to a shell-side domain to form a shell-and-tube heat exchanger^{2,19}. Whilst this is the final application envisaged, the scope of this paper is restricted to a single tube.

Deposition, ageing and cleaning models

In this section first some classic deposition and ageing models are re-cast in the new multicomponent, reaction engineering framework presented here. Second, fouling and cleaning are defined within an overall rate of deposition model and some rate- and state-dependent models are presented for the cleaning operations.

In this work organic fouling is considered as the only fouling mechanism, thus the deposit is simply composed of two pseudo-components (NC=2), gel and coke, and ageing of gel to produce coke is the only reaction (NR=1). An example of deposits formed by organic and multiple inorganic species is presented elsewhere⁴⁰.

Fouling Deposition model

In the approach presented, fouling rates are defined as mass fluxes of material into or leaving the deposit. Consequently, classic fouling rate equations based on thermal resistance are not directly applicable. An example of a classic fouling equation for organic fouling is the “threshold” model introduced by Panchal et al.⁴¹:

$$\frac{dR_f}{dt} = \alpha Re^{-0.66} Pr^{-0.33} \exp\left(\frac{-E_f}{RT_{film}}\right) - \gamma \tau_w \quad (26)$$

where α , E_f and γ are adjustable parameters dependent on the crude type. The general functional form of the threshold model is adopted and used here to estimate the *local fouling net deposition*:

$$n_{f,gel}(z) = \alpha' Re(z)^{-0.66} Pr(z)^{-0.33} \exp\left(\frac{-E_f}{RT_{film}(z)}\right) - \gamma' \tau_w(z) \quad (27)$$

where $n_{f,gel}$ is the net mass flux of freshly deposited gel (at each z coordinate). Coke is assumed not to deposit at the layer boundary, hence:

$$n_{f,coke}(z) = 0 \quad (28)$$

There is a formal equivalence to Eq. (26) parameters:

$$\alpha' = \lambda_{gel}\rho_{gel}\alpha \quad \left[\frac{kg}{m^2s} \right] \quad (29)$$

$$\gamma' = \lambda_{gel}\rho_{gel}\gamma \quad \left[\frac{kg}{m^2sPa} \right] \quad (30)$$

The new parameters have units of mass transfer coefficients or surface reactions, which is coherent with the overall reaction engineering approach used here. However, there is no reason why numerical values of parameters calculated from overall thermal resistance should translate into appropriate values for a deposition model of the same form. In practice, parameters in Eq. 27 should be re-evaluated by fitting primary data to the full dynamic model described. Ideally, this semi-empirical approach should be substituted by more fundamental mechanistic models relating deposition rate to the local operating conditions, concentration of foulant (or precursor) and crude oil physical properties.

Kinetic Ageing Model for Organic Deposits

High temperature ageing of hydrocarbons has been observed to involve changes in chemical composition⁴². This is represented as a single first order chemical reaction by which gel is transformed into coke:

$$r_a(z, \tilde{r}_l) = k_a(z, \tilde{r}_l)\rho_{gel}x_{l,gel}(z, \tilde{r}_l) = k_a(z, \tilde{r}_l)c_{L,gel}(t, \tilde{r}_l) \quad \left[\frac{kg}{m^3s} \right] \quad (31)$$

where:

$$k_a(z, \tilde{r}_l) = A_a \exp\left(-\frac{E_a}{R_g T_l(z, \tilde{r}_l)}\right) \quad [s^{-1}] \quad (32)$$

The stoichiometric coefficients for the ageing reaction are +1 for coke (formation) and -1 for gel (consumption), and 0 for any other components.

If there are no other species than gel-coke present, Eq. (10) simplifies to:

$$\lambda_l(z, \tilde{r}_l) = x_{l,gel}(z, \tilde{r}_l)\lambda_{gel} + (1 - x_{l,gel}(z, \tilde{r}_l))\lambda_{coke} \quad (33)$$

Solving the equation for the volume fraction of gel gives:

$$x_{l,gel}(z, \tilde{r}) = \frac{\lambda_l(z, \tilde{r}_l) - \lambda_{coke}}{\lambda_{gel} - \lambda_{coke}} \quad (34)$$

The relationship above is the definition of “youth” variable in previous works^{12,13}, hence $x_{l,gel} \equiv y$ and the equivalence between Eq. (31) and the ageing kinetics in those references is:

$$r_a/\rho_{gel} = k_a y = -\frac{dy}{dt} \quad [s^{-1}] \quad (35)$$

Due to a lack of experimental data, values for the kinetic constants A_a and E_a have been proposed based on parametric studies, defining three degrees of ageing according to the rate of change: slow, intermediate and fast. As the kinetic model is the same, those parameter values can be reused.

Modelling Fouling-Cleaning Processes

The thickness of the deposit layer at each point z along the tube will change according to the mass of material either depositing or leaving the fouling layer. During normal refining operation, the processes affecting the layer will be related to fouling mechanisms, such as deposition and suppression/removal. On the other hand, during cleaning the processes affecting the layer are related to chemical or mechanical removal. In this section, a general formulation is proposed to simulate fouling-cleaning cycles using the modelling framework presented in the previous section.

Obviously, fouling and cleaning processes do not happen simultaneously. However, a continuous transition between fouling and cleaning periods is desirable in a dynamic simulation. For this purpose, a formulation using binary variables to select between operation (fouling) or cleaning is introduced. In general terms, the rate of change in thickness is defined as:

$$\dot{\delta}_l(z) = (1 - b_{clean}) \sum_i^{NC} \frac{1}{\rho_i} n_{f,i}(z) - \sum_{k=1}^{NCl} b_k \frac{1}{\rho_l(z, 1)} n_{cl,k}(z) \quad (36)$$

where $n_{f,i}$ is the net mass flux of species i deposited, $n_{cl,k}$ is the cleaning rate for method k (in terms of mass flux removed). b_{clean} a 0-1 variable indicating whether any cleaning is active and b_k is a binary variable which

defines whether the cleaning action k is taking place ($b_k=1$) or not ($b_k=0$). N_{Cl} indicates the number of cleaning methods considered, of which at most one at a time is used, i.e. $b_{clean} = \sum_{k=1}^{N_{Cl}} b_k \leq 1$. During a cleaning period, fouling and other physical-chemical transformations (such as ageing) are stopped, and the cleaning rate is activated. In order to stop any internal reactions in the model, the right hand side in the mass balances (Eq. 16) is multiplied by $(1 - b_{clean})$.

As noted in the introduction, cleaning of fouled heat exchangers is usually carried out either mechanically or with the use of chemicals. A mechanical cleaning normally but not always produces a complete cleaning, while a chemical cleaning can produce a complete cleaning if applied early enough, as shown later in the case study. This is schematically represented in Figure 3, where each cartoon from left to right represents the layer depth at successive times.

Rate models are proposed for chemical cleaning and complete mechanical cleaning. The extent of cleaning depends on the cleaning method, the properties of the layer at that particular time, and the time allowed for cleaning. This is captured by defining a termination condition that depends on the cleaning method and a rate constant.

The duration of the cleaning can be either fixed or condition-based. With fixed time, the duration of the cleaning is externally imposed by an operation schedule. In order to simulate this cleaning mode, the rate constant is chosen a priori as a sufficiently high value that ensures reaching the termination condition within the specified time in all cases to be encountered, but not so high that it would create numerical issues. The evolution of deposit thickness for fixed-time cleaning is shown in Figure 4(a). Conversely, with condition-based mode the cleaning period lasts until the termination condition is reached, within certain absolute tolerance, as shown Figure 4(b). This modelling approach for cleaning has the advantage of allowing seamless simulation of fouling-cleaning periods. In addition, the same cleaning rate models can be used to simulate both fixed-time and condition-based cleaning modes.

A chemical cleaning method k (referred to with subscript Ck) is defined by two characteristic parameters: a cleaning rate constant, k_{Ck} [in units of $\text{kg}/\text{m}^2\text{s}$], and the maximum fraction of coked deposits, $x_{Ck, coke}$, that can be removed by the cleaning method. The cleaning rate, $n_{Cl, Ck}$, is defined as:

$$n_{Cl,Ck} = k_{Ck} (x_{Ck,coke} - x_{l,coke}|_{\bar{r}_l=1}) \quad (37)$$

$x_{Ck,coke}$ represents the efficacy of method k in removing the deposits and $x_{l,coke} (\bar{r}_l=1)$ is the local concentration of coke at the surface of the deposit. The above model assumes that the presence of coke is the main factor limiting the cleaning efficacy. The condition may vary for distinct types of cleaning agents. The value of the characteristic parameters ($x_{Ck,coke}$ and k_{Ck}) is to be calculated from measurements, when available. The above model is a first order model with respect to composition. The cleaning rate smoothly tends to zero as the termination condition $x_{Ck,coke}$ is approached due to the increased difficulty in removing the remaining material. Once the condition is reached, with certain tolerance, the cleaning rate stays at a value of approximately zero until the end of the period. If the fixed time specified is longer than required, more cleaning fluid and time than necessary are used leading to additional cost, but no further cleaning is achieved. If the specified fixed time is too short, the opportunity to remove some more deposit is lost.

Alternatively, if the ageing process and cleaning method are well characterized, it is possible to define a schedule with a condition-based termination of the cleaning interval. The chemical cleaning will be stopped as soon as the condition is reached, or even earlier if that entails an economic benefit. Other condition-based models, considering for instance zeroth order kinetics (constant rate) or additional features (e.g. initiation period), could be considered.

For complete mechanical cleaning (subscript M), the cleaning time, t_M , is typically fixed. A rate of cleaning is defined to ensure full cleaning is achieved in that time as:

$$n_{Cl,M} = k_{Cl,M} \delta_l \quad (38)$$

where k_M is a rate constant [in units $\text{kg}/\text{m}^3\text{s}$]. The model is first order with respect to the thickness. As the deposit becomes smaller it becomes more difficult to remove (cleaning rate decreases with thickness). Once the deposit is completely removed, the cleaning rate becomes essentially zero and stays at that value until the end of the allocated fixed cleaning time. In the case of mechanical cleaning, the cleaning time t_M would include operations such as dismantling, transportation (if carried out off-site), and reassembling the exchanger, for which a fixed time is required irrespective of fouling state. More sophisticated models, combining fixed time for operations and condition-based time for cleaning, are easily considered. For particular cases in which mechanical cleaning might only partially remove the layer, an expression of the

form of Eq. (37) would be more appropriate. The advantage of a rate-based model is that incomplete cleaning could then be modelled even for a mechanical cleaning, if too hurried.

It should be noted that the framework allows for any combination of fixed time or condition based cleaning. The presented models are just examples.

Application: Fouling-Cleaning Cycle

Among the potential applications of the novel model, a case study is presented for fouling and cleaning processes. Organic fouling is considered as the only fouling mechanism. The parameters for the tube geometry, operating conditions, crude oil physical properties, fouling rate, ageing rate and cleaning rates are shown in Table 2. These parameters are representative of typical refinery exchangers¹³. UWT operation mode is assumed. The conductivities of gel and coke are also reported in Table 2. Cleaning constants and a value of $x_{Ck,coke}$ are assumed for illustration purposes (Chemical method C1). A fixed time is specified for a mechanical cleaning, with both fixed and condition-based time for chemical cleaning.

First, a single chemical cleaning of an organic fouling deposit is simulated. The concentration profiles and consequent thermal and hydraulic effects at key times are discussed. The importance of the timing of the cleaning is highlighted. Finally, different types of cleaning methods are simulated in an example of cleaning cycle.

Chemical Cleaning: Concentration Profile and thermal impact

An operation is considered consisting of three periods: (i) 6 months of operation starting from a clean tube during which fouling occurs and the layer builds up; (ii) a single chemical cleaning (fixed time), with layer thickness reduction; and (iii) subsequent operation for another 6 months during which fouling resumes. The fouling layer thickness at the midpoint of the tube ($z=3.05\text{m}$) evolves over time as shown in Figure 5, where a number of key times (A ... F, discussed later) are also indicated. Time A was chosen so that the deposit thickness is the same as that left after cleaning is completed at time C. The gel and coke concentration profiles through the layer (again at tube midpoint) at the above key times are shown in Figure 6, for periods (i), (ii) and (iii) (left to right). The thickness is represented on the vertical axis and the volume fraction on the horizontal axis.

At time zero (beginning of period i, labelled “ $t = 0$ ” in Figure 6) the deposit thickness is zero and the initial deposit has volume fractions of gel and coke equal 1 and 0, respectively. During period (i), organic material builds up on the inner surface of the tube. The portion of the layer near the deposit surface is mainly composed of gel. The oldest part of the layer, near the wall (bottom of Figure 6) has greater concentration of coke which increases over time. At time A the deposit has a thickness of 0.63 mm; the volume fractions of gel and coke near the wall have become 0.33 and 0.67, respectively. The deposit keeps growing and ageing. At time B, the end of period (i), the thickness is 1.19 mm, and the volume fractions of gel and coke at the wall are 0.09 and 0.91, respectively. Given the higher conductivity of coke, the ageing process gradually increases the effective conductivity of the fouling layer. However, the overall thermal resistance increases over time as a result the continuous addition of less conductive fresh material on top of the older deposit and deeper layer. This effect is thermally dominant with respect to the increase in conductivity due to ageing, resulting in decreasing temperature at the surface of the deposit, as shown in Figure 7(a) for the transition A→B. The deposit surface temperature that was 220.5°C at time A decreased to 214.5°C at time B. As ageing progresses the temperature profile within the layer acquires a significant curvature, with a very steep gradient near the top of the layer.

The concentration profiles noted result in corresponding radial conductivity profiles that represent the key influence on the thermal behaviour of the fouling layer. For the binary gel-coke system considered here, the conductivity profile has the same shape as the coke fraction profile and is not shown. The layer conductivity at any one point varies between that of gel (at 0% coke fraction) and that of coke (for 100% of coke fraction). The effect of ageing rate on the thermal behaviour of the fouling deposit has been studied in detail elsewhere¹³.

At time B, after 6 months, a chemical cleaning characterised by parameters in Table 2 is carried out (period ii, ending at time C). No further ageing occur during cleaning, therefore the concentration profiles in the material deposited remains the same as at time B. The thickness of the layer gradually decreases as a result of the removal of material (according to Eq. 37) and the gel fraction at the top of the remaining layer decreases, according to the concentration profile left at each depth at time B.

Removal continues until the concentration of coke at the top approaches the maximum removable by this specific cleaning method (0.5 in this case) although the cleaning time here was fixed as a full day. This

is shown in Figure 8, where the gel concentration at the deposit surface is plotted against time. The layer remaining at that time has greater coke concentration, hence higher conductivity and higher surface temperature than the layer of the same thickness during period (i), as shown by points C and A in Figure 7(a). Indeed the difference is 10.5°C. For the assumed rate constant, the termination condition is reached (within an absolute tolerance of 0.01) after 9h. This time is significantly lower than the fixed 24h time allocated for the cleaning period. Therefore, a condition-based termination would reduce the time and cost of the cleaning.

At time D (beginning of period iii) normal operation is resumed and fouling starts building-up again on top of the deposit left at the end of the chemical cleaning. The volume fractions of gel and coke at the surface of the deposit layer at time C are 0.5 and 0.5 respectively and far from the concentration of the fresh deposit (volume fraction of gel, coke = 1, 0). The formulation of the boundary condition permits a smooth transition between these concentrations, avoiding numerical issues. Fouling re-start on top of the old deposit results in a sharp change in the concentration at the boundary (Figure 8) and consequently in the concentration radial profile (Figure 9).

This concentration “moving front” remains in place at that radial location (deposit depth = 0.63 mm in the original r domain), and “travels” from $\tilde{r} = 1$ towards lower values of \tilde{r} in the transformed radial domain. This concentration front, shown in Fig. 9, entails a corresponding change in the slope in the temperature profile, as shown in Figure 7(b) at times D and E (20 days after D). As time progresses, however, the difference in the concentration gradient gradually decreases and eventually this effect dissipates. At time F, the end of period (iii), the temperature profile becomes qualitatively similar to that at the end of period (i) (Figure 7(b)).

It is clear that a simple double layer (or treble layer, or finite no. of fixed layers) model is unlikely to capture such dynamic behaviour, which significantly affects temperatures in the layer, heat flux and deposition rates. Capturing these discontinuities in composition, thermal conductivity and temperature within the deposit layer and their evolution over time (formation, change in shape and disappearance) as a function of operating conditions is one of the main contributions of this work.

The complex role of ageing on thermal performance after chemical cleaning may be assessed by comparing the performance of the unit at time C (after cleaning) and time A (during period (i)). In both cases

the deposit thickness is the same (0.63 mm), but at time A the deposit was significantly younger and less coked (Figure 6). The higher layer surface temperature at time C, compared to time A, has two opposite effects: it promotes fouling (negative) and enhances heat transfer to the oil (positive). The simulation results (see Table 3) show that the enhancement in heat flux is the predominant effect, with an increase of 51% at time C with respect to time A. On the other hand, the increase in fouling rate between C and A is only 11%. After cleaning, it takes 92.5 days for the deposit to reach again the same thickness it had just before cleaning ($\delta_{l,B}$). However, it takes 107.5 days for the heat flux to reach again its pre-cleaning value ($q''_{l,B}$). Consequently, ageing partly offsets the negative thermal effect of fouling.

Timing and effectiveness of the Chemical Cleaning

The timing of a cleaning plays an important role on the improvement in thermal and hydraulic performance achieved. Here, the previous operation (single chemical cleaning of type C1 ($x_{C1,coke}=0.5$) after 6 months) is repeated but with cleaning at months 3 or 9. The impact on deposit thickness and heat duty over time is shown in Figure 10(a) and (b), respectively. The thermo-hydraulic performance is shown in Figure 10(c) on a TH- λ plot. This representation, which is explained in detail elsewhere⁴³, shows simultaneously the impact of fouling on heat duty and pressure drop (both normalized with respect the corresponding values in clean conditions). Some other performance figures of interest are also displayed in Table 3.

The thickness of the deposit removed (in absolute value) is similar in the three cases. The improvement in heat duty, however, is clearly greater when the cleaning is carried out earlier. A cleaning performed after 3 months recovers 44.4% of the initial (clean) heat duty, whilst the same activity carried out after 9 months only recovers 16.9% of the clean heat duty (calculations are reported in Table 3). This is a result of the fast drop in heat duty as fouling builds up. It must be highlighted that the results are a function of the operation mode.

Regarding the hydraulic performance, the improvement in pressure drop (ΔP) is more noticeable when cleaning is performed later (Table 3), a result of the non-linear dependence of pressure drop on flow area. This is shown in Figure 10(c), where the distance between B (before cleaning) and C (after cleaning) on the horizontal axis gives the improvement in pressure drop.

Comparing performance at times C and A, as in the previous section, in all cases the increase in heat flux (positive effect) is dominant compared to the increase in fouling rate (negative effect), although the effects become comparable when cleaning is performed early. Earlier cleaning leads to removal of a greater proportion of deposit, but to faster return to the thickness and thermal performance that pertained before cleaning. On the other hand, the area under the curves in Figure 10(b) clearly shows that the savings in heat duty are greater when cleaning is performed after 3 months compared to later cleaning. This is, again, subject to the operation mode.

Results for cleaning with a less aggressive (C2, $x_{C2,coke} = 0.3$) and a more aggressive (C3, $x_{C3,coke} = 0.7$) chemical after 6 months are also included in Figure 10 and Table 3. It is assumed the same cleaning rate constant applies for C2 and C3 as for C1. As expected, a more aggressive cleaning leads to greater improvement in both thermal and hydraulic performance, whilst the opposite happens when a less aggressive cleaning is used. It takes method C2 less than 8 hours to reach the termination condition (within absolute tolerance of 0.01 on coke fraction) and less than 11 hours for C3, compared to the 9 h for C1. In all cases, the time is much shorter than the allocated 24h fixed time, indicating that 50-65% savings in cleaning time and chemicals could be achieved for the same result. The efficacy of a cleaning is clearly affected by its timing as also shown in Table 3. A later cleaning leaves a higher proportion of deposit inside the tube, although it achieves a large pressure drop reduction. A simulation without cleaning is used to map the potential efficacy of cleaning, in terms of proportion of removable layer. Figure 11 shows the iso-lines for volume fraction of coke as a function of time and the dimensionless radial coordinate. For chemical agent C1 ($x_{C1,coke} = 0.5$) the 0.5 iso-line separates the removable layer ($x_{coke} < 0.5$, above the line in the figure), from the non-removable layer ($x_{coke} \geq 0.5$, shaded area below the line). Since the plot is in terms of the dimensionless radial coordinate, the difference on the vertical axis between the line for $x_{coke} = 0.5$ and $\tilde{r}_l = 1$ at any time gives the proportion of layer that can be removed, which multiplied by the thickness at that particular time gives the actual thickness. An interesting result from the figure is that if the chemical cleaning is carried out before approximately 50 days, it would result in complete removal of the deposit, and repeated cleaning at this frequency would be sufficient to completely avoid the need for mechanical cleaning. Of course, whether this is the best option will depend on an economic analysis. This analysis has been performed on the midpoint of the tube, which gives approximately average results between the two tube ends. In heat exchangers, where

the temperature of the shell fluid changes significantly along the exchanger, the analysis should be carried out at the hottest end where more acute fouling and ageing are expected.

Figure 11 also shows the time evolution of the concentration profile. Focusing on the non-removable portion, after 100 days, for instance, the profile shows a variation in coke content between 0.5 (at the top of the shaded portion) and 0.7 (near the wall). After a year a significant proportion of the deposit has coke concentrations over 0.8-0.9. The results indicate a significant variation in the conductivity of the non-removable deposit over time, which will have a significant effect on the thermal performance of that portion of the layer. Even with the fast ageing of this case study, the average conductivity of the hard deposit remains quite far from that of coke for most of the time. Again, a simple double layer model, where the conductivity of the “hard” deposit is directly considered equal to coke, is likely to incorrectly impact the calculation of heat flux, heat recovered and the trade-offs in the optimization of cleaning schedules.

Condition-based cleaning sequence

The previous section has shown that the duration of a chemical cleaning, its immediate efficacy (in terms of extent of removal of deposited material) and its long-lasting effect (balance between promoting fouling and enhancing heat transfer in the following period) are not fixed but depend on the state of the tube when it is applied.

A combination of different types of cleaning methods is typically used. An example of fouling-cleaning cycle with multiple cleanings is shown in Figure 12: a condition-based chemical cleaning after 100 days, and a fixed-time mechanical cleaning after 275 days. Model parameters are shown in Table 2. After 100 days of operation, starting from a clean tube, a condition-based chemical cleaning (method C1) is applied. Cleaning stops as soon as the cleaning termination conditions is reached (within a tolerance of 0.01), reducing the cleaning time from the previously fixed 24h to only 7h. This restores the heat duty from 31.4% to 75.6% of the clean value. Operation is resumed and continues until the second cleaning is performed. The mechanical cleaning lasts for 5 days (fixed time) and restores the tube from a quite fouled state (heat duty 22% of the clean value) to completely clean conditions. Normal operation takes the tube to the end of the cycle at (assumed fixed) 450 days. This specific schedule, including state-dependent conditions for switching

between operation and cleaning of two types, was simulated with the single dynamic model described in previous sections.

Conclusions

A new dynamic, 2D distributed, first-principles model for the fouling deposit layer inside a tube was presented. The deposit layer is represented as a multi-component solid which may grow or decrease depending on deposition and removal fluxes at a moving boundary between deposit layer and flowing crude oil. The composition within the layer may change according to chemical reactions between the species present. This approach permits decoupling the main processes involved: heat transfer, chemical reactions, and deposition/removal; this enables the individual study of the various effects and their assembly within a single, integrated model that captures the complex dynamic interactions involved.

A Lagrangian transformation of the mass and energy balances, together with an appropriate formulation of the boundary condition and choice of solution method, permit handling the moving boundary condition and the correct conveying of information from the boundary layer through the radial direction even in the presence of discontinuities. These key features of the deposit layer model overcome several assumptions of previous work^{2,13} (comparison provided in Appendix II) and broaden the range of practical applications:

- a) Substitution of an ageing model specific for thermal fouling by a mass balance leads to a general formulation, allows handling multi-component systems and different reaction mechanisms.
- b) The ageing model¹³ was strictly valid for linear growth of the deposits only. The present treatment requires no such assumption.
- c) It is possible to simulate partial removal without losing the all-important time-temperature-composition history at each point of the deposit layer, and then resume subsequent (fouling) operation.
- d) It is possible to change the rate and composition of fresh deposition fluxes at any time during a simulation (as a result of change in fouling deposition mechanism, flowing oil composition, relative rates of deposition of different species, etc.) without affecting the layer preceding history.

- e) It is possible to model various types of cleaning activities, including those where cleaning time and removal effectiveness are not fixed a priori but are condition- and extent-based. Some initial cleaning models were presented in this paper.
- f) It is possible to switch seamlessly within the same dynamic simulation between operation (fouling) and any type of cleaning, in any order (i.e. operation-cleaning cycles and schedules).
- g) The model enables, and lends itself naturally to the formulation of fouling-cleaning cycle optimisation as a dynamic optimisation problem.

As in earlier work², the deposit layer domain was implemented in a tube model comprising three domains: tube wall, fouling layer, and oil flow (tube-side). The case study presented, albeit for a single tube, demonstrated that different extent of cleaning can be considered by relating the effectiveness of a cleaning method to the degree of coking. The detailed simulation permits evaluating opposite effects of ageing/cleaning, such as the enhancement in heat transfer and fouling rate, on long term thermal and hydraulic performance.

The effectiveness of a chemical cleaning was shown to be dependent on the time it is applied and on the layer conditions at that time. It was shown that (for a tube) simulation of condition-based chemical cleaning also permits mapping the concentration profile over time and finding the maximum time for which a chemical cleaning would be as effective as a more expensive mechanical cleaning. It is postulated this analysis could be extended to whole heat exchangers.

The work presented provides, to the authors' knowledge, the most comprehensive model to date to simulate fouling, different cleaning methods and whole fouling-cleaning cycles within the same dynamic model. It is envisaged it will be easily incorporated in full scale models of heat exchangers and preheat trains^{2,19} and used to simulate industrially sized equipment and time-scales, to estimate fouling, ageing and cleaning parameters from experimental data, and in optimization formulations. With a single model in place, we are now in the position of addressing cleaning cycle optimisation as a dynamic optimisation problem. An accurate evaluation of the dynamic behaviour of the units undergoing fouling and the effect of cleaning, such as that provided in this work, is of paramount importance to correctly evaluate the economic trade-off and assist in the decision of the type and timing of cleaning. Such applications will be covered in later publications. The approach presented is general, not specific to crude oil fouling and can be easily adapted to

different geometries and fouling mechanisms, thus it may be applied to other fouling systems. Examples in other petrochemical processes include coke deposition in transfer line exchangers and furnaces in steam crackers^{42,44,45}, wax deposition in pipelines, etc. Examples in other industries include food (e.g. milk fouling⁴⁶) and water transportation (formation of salt scales).

Systematic tuning and validation of the model presented here would involve: a) the design of controlled experiments for the detailed study of the deposition and removal rates of individual fouling species and species in combination; b) a study of the evolution over time of the fouling deposit under relevant operating conditions (e.g. ageing or other transformations); c) validation using experiments in which, for instance, the type of foulant is varied at different stages of the experiment or in which the layer is disrupted at some point (e.g. by partial removal due to shear or use of a cleaning agent). Experimental results thus obtained can be used to validate the model's ability to track local history of the deposit due to deposition, removal or transformation by comparing the final composition of the layer to the distribution predicted by the model.

In the case of crude oil fouling, more experimental data are required to establish reliable ageing kinetics, its impact on the thermal and mechanical properties of the layer, and the ability of different cleaning agents to remove organic deposits. The new model itself can be used to guide the design of experiments aimed at achieving a better understanding of the mechanisms limiting deposition, as discussed in reference⁴⁷, where an example of experiment to distinguish between suppression and removal mechanisms is proposed. Good quality experimental data can be obtained from controlled experiments using state-of-the-art fouling rigs, such as those under development at Imperial College London⁴⁸. Thermo-hydraulic measurements and analytical characterization of deposit thus produced can be used in conjunction with the analysis of deposits from refinery heat exchangers to validate and, if necessary, improve models for deposition, removal and ageing.

Acknowledgments

This research was partially performed under the UNIHEAT project. EDB and SM wish to acknowledge the Skolkovo Foundation and BP for financial support. The support of Hexxcell Ltd, through provision of Hexxcell Studio™, is also acknowledged.

Notation

A_a	=	Ageing pre-exponential factor, s^{-1}
API	=	API gravity
b_{clean}	=	Sum of cleaning binary variables for all cleaning methods
b_k	=	Cleaning binary variable for method k
c	=	Mass concentration, $kg\ m^{-3}$
C_p	=	specific heat capacity, $J\ kg^{-1}\ K^{-1}$
$CFDM$	=	Centred finite discretization method
D	=	Diffusion coefficient, $m^2\ s^{-1}$
E_a	=	Ageing activation energy, $J\ mol^{-1}$
E_f	=	Fouling deposition activation energy, $J\ mol^{-1}$
$FFDM$	=	Forward finite discretization method
h	=	Tube-side heat transfer coefficient, $W\ m^{-2}\ K^{-1}$
k_a	=	Ageing kinetic constant, s^{-1}
k_{Ck}	=	Chemical Cleaning rate constant of method k
k_M	=	Mechanical Cleaning rate constant
L	=	Tube length, m
$MeABP$	=	Mean average boiling point, $^{\circ}C$
$n_{Cl,k}$	=	Cleaning rate of method k , $m^3\ m^{-2}\ s^{-1}$
$n_{f,i}$	=	Fouling rate of component i , $m^3\ m^{-2}\ s^{-1}$
NC	=	Number of components
NCl	=	Number of cleaning methods
NR	=	Number of reactions
PHT	=	Pre-heat train
Pr	=	Prandtl number
Q	=	Heat duty, W
q''	=	Heat flux, $W\ m^{-2}$

R_{flow} = Flow radius, m

RI = Inner tube radius, m

RO = Outer tube radius, m

Re = Reynolds number

R_f = Fouling resistance, $m^2 K W^{-1}$

R_g = Ideal gas constant, $J mol^{-1} K^{-1}$

r = Radial coordinate, m

\tilde{r} = Dimensionless radial coordinate

r_j = Rate of reaction j, $kg m^{-3} s^{-1}$

T = Temperature, K

T_{film} = Tube-side film temperature, K

t = Time, s

UWT = Uniform wall temperature

x = Volume fraction, $m^3 m^{-3}$

$x_{Ck,coke}$ = Maximum fraction of coked deposit removable by method Ck

y = Youth variable

z = Axial coordinate, m

Greek letters

α = Deposition constant, $m^2 K J^{-1}$

α' = Modified deposition constant, $kg m^{-2} s^{-1}$

γ = Suppression constant, $m^4 K J^{-1} N^{-1}$

γ' = Modified suppression constant, $kg m^{-2} s^{-1} Pa^{-1}$

ΔP = Pressure drop, Pa

ξ = Boundary condition smoothing parameter, m

δ_l = Fouling layer thickness, m

$\dot{\delta}_l$ = Rate of change of fouling layer thickness, $m s^{-1}$

ρ = Density, kg m⁻³

λ = thermal conductivity, W m⁻¹ K⁻¹

ν_{ij} = Stoichiometric coefficient for component i in reaction j

$\nu_{38^\circ\text{C}}$ = kinematic viscosity at 38°C, mm² s⁻¹

τ_w = Wall shear stress, N m⁻²

Subscripts

0 = Clean conditions

a = Ageing

Ck = Chemical cleaning type k

Cl = Cleaning

i = Inner, component number

in = Inlet

j = Reaction number

l = Fouling layer

M = Mechanical cleaning

o = outer

t = Tube-side flow

w = Tube wall

References

1. Coletti F, Joshi HM, Macchietto S, Hewitt GF. Introduction to Crude Oil Fouling. In: Coletti F, Hewitt GF, eds. *Crude Oil Fouling: Deposit Characterization, Measurements, and Modeling*. Gulf Professional Publishing; 2015.
2. Coletti F, Macchietto S. A Dynamic, Distributed Model of Shell-and-Tube Heat Exchangers Undergoing Crude Oil Fouling. *Ind Eng Chem Res*. 2011;50(8):4515–4533.
3. Yeap BL, Wilson DI, Polley GT, Pugh SJ. Mitigation of crude oil refinery heat exchanger fouling through retrofits based on thermo-hydraulic fouling models. *Chem Eng Res Des*. 2004;82(1):53–71.

4. Ebert WA, Panchal CB. Analysis of Exxon crude-oil-slip stream coking data. In: Panchal CB, ed. *Fouling Mitigation of Industrial Heat-Exchange Equipment*. San Luis Obispo, California (USA): Begell House; 1995:451–460.
5. Kern DQ, Seaton RE. A theoretical analysis of thermal surface fouling. *Brit Chem Eng*. 1959;4(5):258–262.
6. Crittenden BD, Kolaczowski ST, Downey IL. Fouling of Crude Oil Preheat Exchangers. *Trans IChemE, Part A, Chem Eng Res Des*. 1992;70:547–557.
7. ESDU. *Heat exchanger fouling in pre-heat train of a crude oil distillation unit, ESDU Data Item 00016*. London; 2000.
8. Knudsen JG, Hays GF. Use of Operating Conditions to Mitigate Fouling of Heat Exchangers. In: Panchal CB, ed. *Fouling mitigation of industrial heat-exchange equipment International conference*. San Luis Obispo, California (USA): Begell House, New York; 1995.
9. Epstein N. A model for the initial chemical reaction fouling rate for flow within a heated tube, and its verification. In: Hewitt GF, ed. *10th Int. Heat Transfer Conf*. Rugby: IChemE; 1994:225–229.
10. Ishiyama EM, Paterson WR, Wilson DI. Thermo-hydraulic channelling in parallel heat exchangers subject to fouling. *Chem Eng Sci*. 2008;63(13):3400–3410.
11. Epstein N. Thinking about Heat Transfer Fouling : A 5 × 5 Matrix. *Heat Transf Eng*. 1983;4(1):43–56.
12. Ishiyama EM, Coletti F, Macchietto S, Paterson WR, Wilson DI. Impact of Deposit Ageing on Thermal Fouling : Lumped Parameter Model. *AIChE J*. 2010;56(2):531–545.
13. Coletti F, Ishiyama EM, Paterson WR, Wilson DI, Macchietto S. Impact of Deposit Aging and Surface Roughness on Thermal Fouling : Distributed Model. *AIChE J*. 2010;56(12):3257–3273.
14. Crittenden BD, Kolaczowski ST. Energy savings through the accurate prediction of heat transfer fouling resistances. In: O’Callaghan P. W., ed. *Energy for industry*. Oxford: Pergamon Press; 1979:257–266.
15. Nelson WL. Fouling of heat exchangers. *Refin Nat Gasol Manuf*. 1939;13(7):271–276.
16. Nelson WL. Fouling of heat exchangers. Part II. *Refin Nat Gasol Manuf*. 1939;13(8):292–298.
17. Atkins GT. What to do about high coking rates. *Petro/Chem Eng*. 1962;34(4):20–25.
18. Ishiyama EM, Paterson WR, Wilson DI. Exploration of Alternative Models for the Aging of Fouling Deposits. *AIChE J*. 2011;57(11):3199–3209.
19. Hexxcell Ltd. Hexxcell Studio. 2015. Available at: <http://www.hexxcell.com>.
20. Coletti F, Macchietto S. Refinery Pre-Heat Train Network Simulation Undergoing Fouling: Assessment of Energy Efficiency and Carbon Emissions. *Heat Transf Eng*. 2011;32(3-4):228–236.
21. Coletti F, Macchietto S, Polley GT. Effects of fouling on performance of retrofitted heat exchanger networks: A thermo-hydraulic based analysis. *Comput Chem Eng*. 2011;35(5):907–917.

22. Diaz-Bejarano E, Coletti F, Macchietto S. Impact of Crude Oil Fouling Composition on the Thermo-Hydraulic Performance of Refinery Heat Exchangers. In: *11th International Conference on Heat Transfer, Fluid Mechanics and Thermodynamics*. Kruger National Park, South Africa; 2015.
23. Mozdianfard MR, Behranvand E. A field study of fouling in CDU preheaters at Esfahan refinery. *Appl Therm Eng*. 2013;50(1):908–917.
24. Sileri D, Sahu K, Ding H, Matar OK. Mathematical modelling of asphatenes deposition and removal in crude distillation units. In: Müller-Steinhagen H, Malayeri MR, Watkinson AP, eds. *Int. conf. on heat exchanger fouling and cleaning VIII*. Vol 2009. Schlading, Austria; 2009:245–251.
25. Yang J, Matar OK, Hewitt GF, Zheng W, Manchanda P. Modelling of fundamental transfer processes in crude-oil fouling. In: *15th International Heat Transfer Conference, IHTC-15*. Kyoto, Japan; 2014.
26. Bayat M, Aminian J, Bazmi M, Shahhosseini S, Sharifi K. CFD modeling of fouling in crude oil preheaters. *Energy Convers Manag*. 2012;64:344–350.
27. Yang M, Crittenden B. Use of CFD to Determine Effect of Wire Matrix Inserts on Crude Oil Fouling Conditions. *Heat Transf Eng*. 2013;34(8-9):769–775. doi:10.1080/01457632.2012.741506.
28. Yang M, Crittenden B. Fouling thresholds in bare tubes and tubes fitted with inserts. *Appl Energy*. 2012;89(1):67–73.
29. Haghshenasfard M, Hooman K. CFD modeling of asphaltene deposition rate from crude oil. *J Pet Sci Eng*. 2015;128:24–32.
30. Müller-Steinhagen H, Malayeri MR, Watkinson a. P. Heat Exchanger Fouling: Mitigation and Cleaning Strategies. *Heat Transf Eng*. 2011;32(3-4):189–196.
31. Joshi HM. Analysis of Field Fouling Deposits from Crude Heat Exchangers. In: Coletti F, Hewitt GF, eds. *Crude Oil Fouling: Deposit Characterization, Measurements, and Modeling*. Gulf Professional Publishing; 2015.
32. Diaby LA, Lee L, Yousef A. A Review of Optimal Scheduling Cleaning of Refinery Crude Preheat Trains Subject to Fouling and Ageing. *Appl Mech Mater*. 2012;148-149:643–651.
33. Ishiyama EM, Paterson WR, Wilson DI. Optimum cleaning cycles for heat transfer equipment undergoing fouling and ageing. *Chem Eng Sci*. 2011;66(4):604–612.
34. Pogiatzis T, Wilson DI, Vassiliadis VS. Scheduling the cleaning actions for a fouled heat exchanger subject to ageing: MINLP formulation. *Comput Chem Eng*. 2012;39:179–185.
35. Pogiatzis T, Ishiyama EM, Paterson WR, Vassiliadis VS, Wilson DI. Identifying optimal cleaning cycles for heat exchangers subject to fouling and ageing. *Appl Energy*. 2012;89(1):60–66.
36. Singh P, Venkatesan R, Fogler HS, Nagarajan NR. Morphological evolution of thick wax deposits during aging. *AIChE J*. 2001;47(1):6–18.
37. Wang J, Carson JK, North MF, Cleland DJ. A new structural model of effective thermal conductivity for heterogeneous materials with co-continuous phases. *Int J Heat Mass Transf*. 2008;51(9-10):2389–2397.

38. Eskin D, Ratulowski J, Akbarzadeh K. A model of wax deposit layer formation. *Chem Eng Sci.* 2013;97:311–319.
39. Eskin D, Ratulowski J, Akbarzadeh K. Modelling wax deposition in oil transport pipelines. *Can J Chem Eng.* 2014;92(6):973–988.
40. Diaz-Bejarano E, Coletti F, Macchietto S. Beyond Fouling Factors: A Reaction Engineering Approach to Crude Oil Fouling Modelling. In: *Heat Exchanger Fouling and Cleaning XI*. Enfield, Ireland; 2015.
41. Panchal CB, Kuru WC, Liao CF, Ebert WA, Palen JW. Threshold conditions for crude oil fouling. In: Bott TR, ed. *Understanding Heat Exchanger Fouling and its Mitigation*. Lucca, Italy: Begell House; 1997:273–281.
42. Fan Z, Watkinson AP. Aging of carbonaceous deposits from heavy hydrocarbon vapors. *Ind Eng Chem Res.* 2006;45(1):6104–6110.
43. Diaz-Bejarano E, Coletti F, Macchietto S. Detection of changes in fouling behaviour by simultaneous monitoring of thermal and hydraulic performance of refinery heat exchangers. *Comput Aided Chem Eng.* 2015;37:1649 – 1654.
44. Cai H, Krzywicki A, Oballa MC. Coke formation in steam crackers for ethylene production. *Chem Eng Process.* 2002;41:199–214.
45. Van Geem KM, Dhuyvetter I, Prokopiev S, Reyniers MF, Viennet D, Marin GB. Coke formation in the transfer line exchanger during steam cracking of hydrocarbons. *Ind Eng Chem Res.* 2009;48:10343–10358.
46. Georgiadis MC, Rotstein GE, Macchietto S. Modeling and simulation of shell and tube heat exchangers under milk fouling. *AIChE J.* 1998;44(4):959–971.
47. Diaz-Bejarano E, Coletti F, Macchietto S. Crude oil fouling deposition, suppression, removal - and how to tell the difference. In: *Heat Exchanger Fouling and Cleaning XI*. Enfield, Ireland; 2015.
48. Macchietto S. Energy Efficient Heat Exchange in Fouling Conditions: the UNIHEAT Project. In: *Heat Exchanger Fouling and Cleaning XI*. Enfield, Ireland; 2015.
49. PSE. gPROMS. 2015. Available at: <http://www.psenterprise.com/gproms.html>.

Appendix I: Numerical Considerations

The model comprises a system of partial, differential and algebraic equations (PDAE). It is implemented and solved in gPROMS⁴⁹. The partial differentials on space domains are discretized, transforming the PDAE system into a DAE system and integrated using the standard DASOLV solver. The axial and the tube wall radial domains are discretized using a second order Centred Finite Discretization

method (CFDM) with 10 points. For the solution of the layer domain in the radial direction, two main aspects were tested: (1) Discretization method and number of discretization points; (2) Smoothing of the mass balance boundary condition. Although the study of the solution method is based on cleaning, it covers all possible scenarios to be encountered in the application of the model: thickness growth, reduction, fouling re-start after reduction, change in inside-layer concentration due to chemical reaction, and change in the concentration at the boundary

CFDM is generally recommended to handle differential equations with mixed convective and dispersive terms, such as Eq. (15). Forward or backward finite discretization methods (FFDM and BFDM), on the other hand, are generally adequate when handling purely convective equations, such as Eq. (16). However, with the latter the choice of discretization method also depends on the formulation of the boundary condition. Two configurations were tested: CFDM for both heat balance and mass balance; and CFDM for heat balance and FFDM for mass balance (CFDM/FFDM). In the latter, two radial domains and number of discretization points are defined.

i. Layer growth with constant concentration at the boundary.

Both CFDM and CFDM/FFDM successfully handled the simulation of the growing layer. Grids with 500 or more discretization points returned identical results to 6 significant digits in mass fraction (both at top and bottom of the layer) after a year of simulation. An exponential transformation of the grid, such as that used in previous work², was also tested returning satisfactory results. The value of the parameter ξ in Eq. 24 was chosen so that the ageing effect on the concentration at the boundary is negligible. For a value of ξ of 10^{-6} m the mass fraction of gel at the boundary is close to 1 (> 0.999) as it should be. Values of ξ greater than 10^{-6} m lead to the fraction of gel at the boundary being $0.9 \div 0.95$, which is far from correct. Values below 10^{-6} m lead to numerical instability and even failure. Therefore, a value $\xi = 10^{-6}$ is selected.

ii. Layer thickness reduction (cleaning) following growth (deposition)

CFDM successfully handled the switch from a positive to a negative change in thickness. The same results to 6 significant digits in mass fraction (both at top and bottom of the layer) were obtained for uniform grids with over 500 points and for a 150-points grid with exponential transformation. CFDM/FFDM, however, could not handle reduction. Therefore, CFDM is selected for a reduction period.

iii. Layer growth re-start after reduction

The boundary condition in Eq. 24 results useful to smooth the transition from final concentration on the layer boundary after a reduction to the concentration of freshly laid deposit. The speed of this transition depends on the value of ζ . Very small values of ζ may cause numerical problems, and very big values will produce a smooth, easy-to-handle transition but may delay the step return to the fresh concentration. In order to test FFDM method, which fails to simulate removal, a complex strategy is required: FFDM is used when $\delta_1 > 0$ and changed to CFDM when $\delta_1 < 0$. As shown in Figure 13, the transition of concentration at the boundary to the expected value (gel volume fraction=1) is very fast for $\zeta = 10^{-6}$ and becomes of the order of days for greater values. Values of ζ below 10^{-6} lead to numerical difficulties with FFDM/CFDM method. Therefore, a value of 10^{-6} was chosen to maintain both accuracy and numerical stability. On the other hand, with CFDM the transition does not require a change in discretization method, but requires a minimum value of ζ of $5 \cdot 10^{-6}$ to avoid numerical issues.

As discussed in the main text, the step in concentration appears at the layer boundary and gradually moves inside the dimensionless domain. This is shown in Figure 14 for time D, just after deposition re-start, and 6 months later (time F).

With CFDM, the radial concentration profile shows a wavy behaviour. These waves become more pronounced as the number of discretization points is reduced and the step front moves from the boundary to inner locations, as a result of the growth of the layer. This must be avoided since it may lead to instability and convergence problems. On the other hand, the FFDM/CFDM method permits a faster and completely smooth transition in the concentration of the fresh deposit just after re-start. Based on these results the best choice seems to be FFDM/CFDM with $\zeta = 10^{-6}$.

The number of discretization points becomes relevant as the step in concentration moves through the dimensionless domain as a result of the layer growth. As shown in Figure 14(b), the transition seems to become smoother in the inner layers. For this period, an exponential transformation seems inadequate because of the loss in definition of the step as it moves from the boundary to inside of the layer. Consequently, grids with exponential transformation should only be used when the concentration at the boundary is not expected to change. The choice of the number of points will depend on the trade-off between accuracy and simulation time. In the examples presented in this paper, a uniform grid with 2000 points was used.

Appendix II: Model Comparison

The model presented overcomes some of the assumptions and limitations in previous models as discussed in the conclusions. Two aspects relevant to the application example in this paper are discussed below by comparing the simulation results of the ageing model in previous works^{2,13} (referred to as Model I) and the deposit model presented here (referred to as Model II):

a) Calculated ageing and heat flux during deposit build-up:

Results are compared for three values of γ' ($\gamma'_1 = 3.45 \cdot 10^{-9} \text{ kg m}^{-2} \text{ s}^{-1} \text{ Pa}^{-1}$; $\gamma'_2 = 2.4 \cdot 10^{-8} \text{ kg m}^{-2} \text{ s}^{-1} \text{ Pa}^{-1}$; $\gamma'_3 = 4.7 \cdot 10^{-8} \text{ kg m}^{-2} \text{ s}^{-1} \text{ Pa}^{-1}$) for which the growth of the deposit gradually moves away from the linear growth behaviour. Figure 15(a) shows the deposit thickness at the tube midpoint over time for a year of simulation. The inside box shows the difference in heat flux (calculated with reference to the inner tube area) at the tube midpoint between models I and II ($q''_I - q''_{II}$) relative to the total loss of heat flux predicted by model II due to fouling (that is, the difference between heat flux under clean and fouled conditions ($q''_0 - q''_{II}$)), after a year of operation. For γ'_1 (approximately linear growth) the difference in heat flux between the two models is only 0.3% of the total loss of heat flux predicted by Model II. In this case, Model I slightly overpredicts the heat flux compared to Model II (positive error). However, as the layer growth diverges from linear behaviour, the heat flux calculated by Model I becomes gradually smaller than that predicted by Model II. For γ'_3 the difference between the heat flux predicted by the two models is -9% (negative sign due to Model I underpredicting heat flux) of the total heat flux lost due to fouling. This behaviour is consequence of the gel concentration (or youth in the case of Model I) profile, shown in Figure 15(b) for the tube midpoint after a year of simulation. The figure shows that the profile is very similar for γ'_1 . However, as the value of this parameter increases, Model I under-predicts the degree of coking (ageing) of the deposit, which leads to the reduced heat flux. For γ'_3 , the maximum difference in the concentration profile is observed at $\tilde{r}_l = 0.8$, where the degree of coking after 1 year calculated by Model II is 65%, much higher than the 40% calculated by Model I. The Model I underestimation of the degree of coking leads to a heat flux loss underprediction of 2.5 kW/m^2 at the tube midpoint (9% of the total loss of heat flux, as previously commented) an underprediction in the heat duty for the entire tube of 0.9kW at time one year, and an underprediction in cumulative terms of 5MWh of heat transferred to the oil for the entire tube after one year. Considering that

an industrial heat exchanger may have thousands of tubes, the impact is substantial. Therefore, while Model I provides a good approximation of the more rigorous Model II when the growth is approximately linear, it gives a more conservative estimate of the ageing effect when the growth significantly diverges from the linear behaviour. The results show the advantages of using a general formulation relying on mass balances to track the local history of the deposit (such as the provided by model II) for the correct estimation of the effect of fouling and ageing on heat transfer. Approximate models with underlying assumptions on the age of the local elements of the layer (such as the proportional relationship between age and deposit thickness assumed in Model I¹³) may lead to substantial deviations in the estimated degree of coking and heat flux.

b) *Simulation of partial removal of and subsequent re-deposition on an old layer:*

Simulations of fouling build up on a clean surface with a mechanical cleaning action after 6 months of operations were performed so as to compare the responses of Models I and II. The deposit thickness at the tube midpoint is shown in Figure 16(a). The gel volumetric fraction (or youth for Model I) is shown in Figure 16(b) at three key times: just before cleaning (B'), end of cleaning period (C'), and 5 days after the end of the cleaning period (E').

The results show how the mass balance model in Model II is able to track the history of the deposit through the cleaning action and following build-up of fouling: after removal, a small fraction of aged deposit is left (C'); then fresh fouling deposit starts building-up on top of the old deposit, leading to a step in the concentration profile (E'). On the other hand, Model I does not follow the removal of the layer, and ageing continues after C' from the previous youth (gel concentration) radial profile. This demonstrates the ability of Model II to represent both partial and total cleaning, which model I cannot do.

List of Figure Captions

Figure 1. Schematic representation of the model for a single tube

Figure 2. Schematic representation of fouling layer growing between times t_1 (left) and t_2 (right) undergoing reactions, in dimensional coordinates (a) and equivalent layer after Lagrangian transformation (b).

Figure 3. Schematic representation of complete (a) and partial (b) cleaning of a fouling deposit undergoing ageing

Figure 4. Deposit thickness reduction for fixed time (a) and condition-based (b) cleaning. The vertical lines indicate the start and end of the cleaning period

Figure 5. Deposit thickness at the midpoint of the tube ($z = 3.05\text{m}$) over time with a chemical cleaning after 6 months

Figure 6. Thickness and radial (dimensional) concentration profiles at the tube midpoint ($z = 3.05\text{m}$), at key times in periods i, ii and iii (left to right)

Figure 7. Fouling layer temperature profile at the tube midpoint ($z=3,05\text{m}$) at various times

Figure 8. Volume fraction of gel at the deposit layer surface in the tube midpoint during periods i, ii and iii.

Figure 9. Gel fraction profiles against transformed radial coordinate, at the tube midpoint, at time D (just after resumption of fouling) and at time F (6 months later).

Figure 10. Deposit thickness at the tube midpoint ($z= 3.05\text{m}$) (a), heat duty (normalized to clean duty) (b) and Thermo-hydraulic performance (c) for a single chemical cleaning C1 after 3, 6 and 9 months and cleanings C2, C3 after 6 months

Figure 11. Volume fraction of coke as function of the radial coordinate (dimensionless) and time at the tube midpoint ($z= 3.05\text{m}$) for a year without cleaning. The shaded area indicates the non-removable portion by chemical cleaning C1

Figure 12. Deposit thickness at the tube midpoint ($z= 3.05\text{m}$) (a) and heat duty (b) over time for operation during 450 days with condition-based chemical (C1) and fixed-time mechanical cleanings

Figure 13. Effect of ξ on gel volume fraction at the surface of the layer during period (ii) and beginning of (iii) (re-start)

Figure 14. Gel fraction profiles against transformed radial coordinate for various discretization methods, at the tube midpoint, at time D just after resumption of fouling (a) and at time F, 180 days later (b).

Figure 15 Comparison of models I and II for fouling build up considering 3 values of γ' over a year of operation at the tube midpoint ($z=3.05$): (a) deposit thickness and impact on heat flux (in the inside); (b) concentration radial profile after a year.

Figure 16. Comparison of models I and II at the tube midpoint ($z=3.05$) for fouling build up with mechanical cleaning after 6 months: (a) deposit thickness; (b) concentration radial profile at times B', C' and E'.

Table 1. Evolution of models for PHT heat exchangers crude oil fouling deposits over the past 10 years

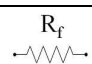
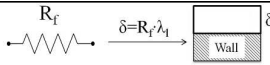
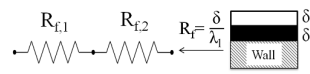
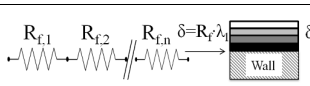
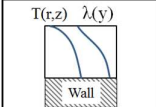
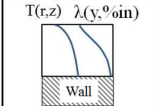
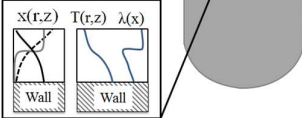
Ref.	Layer description	Thermal effects	Ageing	Composition	Spatial distribution	Change in δ (Hydraulics)	Schematic representation
Traditional (e.g. Refs. 4,6,9,14)	Single, uniform	R_f	-	-	Lumped	-	
Yeap et al. ³	Single, uniform	R_f	-	-	Lumped	Thin slab	
Ishiyama et al. ¹⁸ (based on Nelson ^{15,16})	Double layer	R_f 's in series	As in Ref ² modified as δ exchange between layers	-	Lumped	Thin slab	
Ishiyama et al. ¹²	Multi-layer	R_f 's in series	Gradual decrease in youth "y" (affects λ_f)	Implicit (binary) organic composition	Lumped; multiple layer approximation in radial domain	Thin slab	
Coletti and Macchietto ²	Single, distributed	Heat balance	As in Ref ² extended to distributed system.	Implicit (binary) organic composition	Distributed in axial and radial domains	Moving boundary. Correction for local age of deposit.	
Diaz-Bejarano et al. ²²	Single, distributed	Heat balance	As in Ref ²	As in Ref ² modified to account for inorganics	Distributed in axial and radial domains	As in Ref ²	
This paper	Single, distributed	Heat balance	Chemical reactions	Mass balance. Explicit composition. General reactions	Distributed in axial and radial domains	Moving boundary (Lagrangian Transformation)	

Table 2. Parameters for single tube geometry, operating conditions, crude oil and fouling/cleaning models

Parameter	value	Parameter	value
Tube		Oil Physical Prop.	
RI (mm)	9.93	API	37
RO (mm)	12.70	MeABP ($^{\circ}\text{C}$)	350
L (m)	6.1	$\nu_{38^{\circ}\text{C}}$ (mm^2s^{-1})	4
Operating conditions		Fouling	
UWT ($^{\circ}\text{C}$)	270	α' ($\text{kg m}^{-2}\text{s}^{-1}$)	0.54
T_{in} ($^{\circ}\text{C}$)	200	γ' ($\text{kg m}^{-2}\text{s}^{-1}\text{Pa}^{-1}$)	$3.45 \cdot 10^{-9}$
Flowrate (kg/s)	0.3	E_f (kJ mol^{-1})	28
Cleaning		Ageing	
$x_{CI,coke}$	0.5	E_a (kJ mol^{-1})	50
k_{CI} ($\text{kg/m}^2\text{s}$)	$3.2 \cdot 10^{-4}$	A_a (s^{-1}) (fast)	0.01
t_{CI} (days)	1	λ_{gel} ($\text{W m}^{-1}\text{K}^{-1}$)	0.2
k_M ($\text{kg/m}^3\text{s}$)	0.027	λ_{coke} ($\text{W m}^{-1}\text{K}^{-1}$)	1.0
t_M (days)	5		

Table 3. Comparison of key performance indicators for different timings of the chemical cleaning

Time of Chemical Cleaning (month)	3	6	9	6	6
Type of Cleaning	C1	C1	C1	C2	C3
$\delta_{i,B} - \delta_{i,C}$ (mm)	0.48	0.56	0.58	0.34	0.81
$(\delta_{i,B} - \delta_{i,C})/\delta_{i,B}$ (%)	74.2	47.0	35.0	29.0	68.0
$(Q_C - Q_B)/Q_0$ (%)	44.4	25.1	16.9	14.6	40.2
$(\Delta P_B - \Delta P_C)/\Delta P_0$ (%)	30.4	47.7	67.5	31.4	64.2
Comparison of performance C vs. A ($\delta_{i,A} = \delta_{i,C} = 0.63$ mm)					
$(q''_C - q''_A)/q''_A$ (%)	36.4	51.0	47.6		
$(n_{f,C} - n_{f,A})/n_{f,A}$ (%)	13.1	10.9	7.9		
Time after C to return to performance at B					
Time for $q'' = q''_B$ (days)	75	108	130		
Time for $\delta_i = \delta_{i,B}$ (days)	69.3	92.5	107.8		

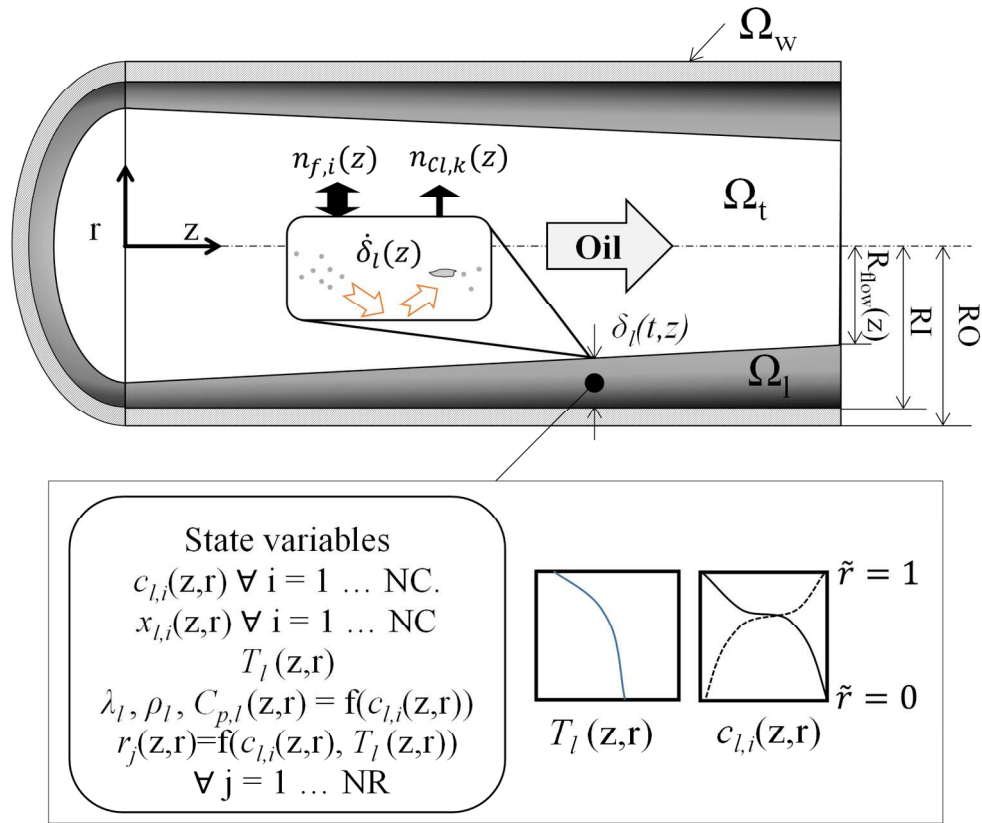


Figure 1. Schematic representation of the model for a single tube.
144x123mm (300 x 300 DPI)

Accep

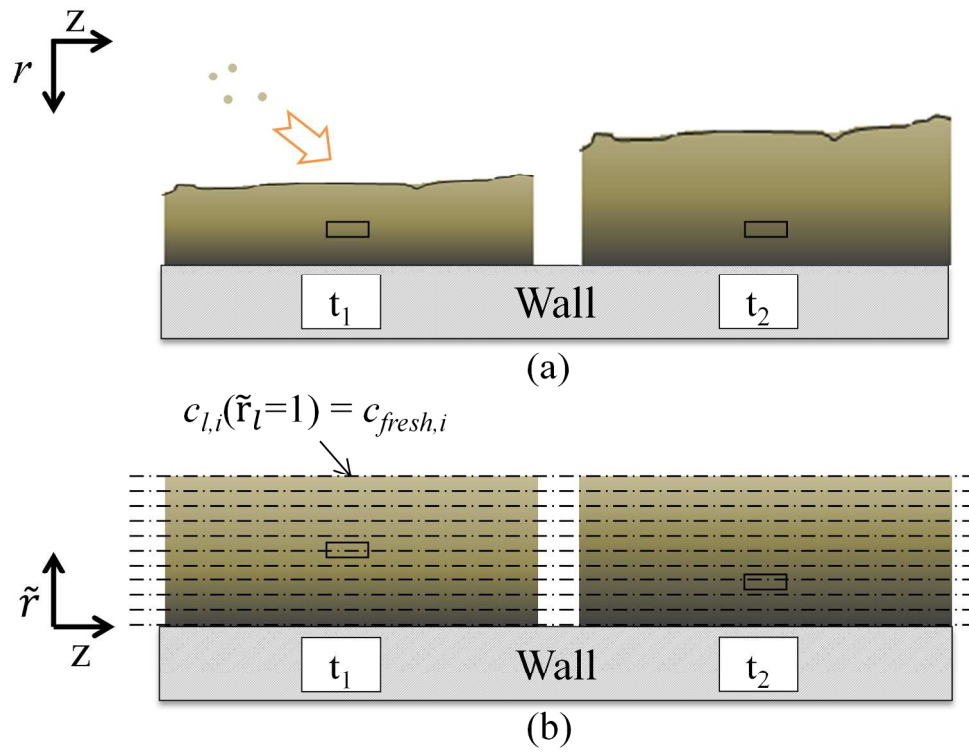


Figure 2. Schematic representation of fouling layer growing between times t_1 (left) and t_2 (right) undergoing reactions, in dimensional coordinates (a) and equivalent layer after Lagrangian transformation (b).

204x162mm (300 x 300 DPI)

Accep

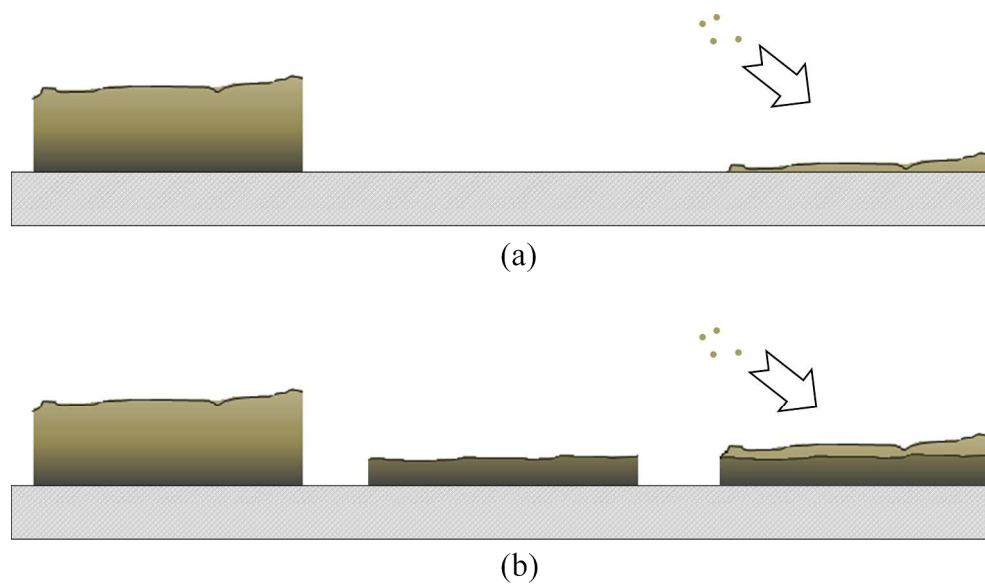


Figure 3. Schematic representation of complete (a) and partial (b) cleaning of a fouling deposit undergoing ageing.
234x137mm (300 x 300 DPI)

Accepted

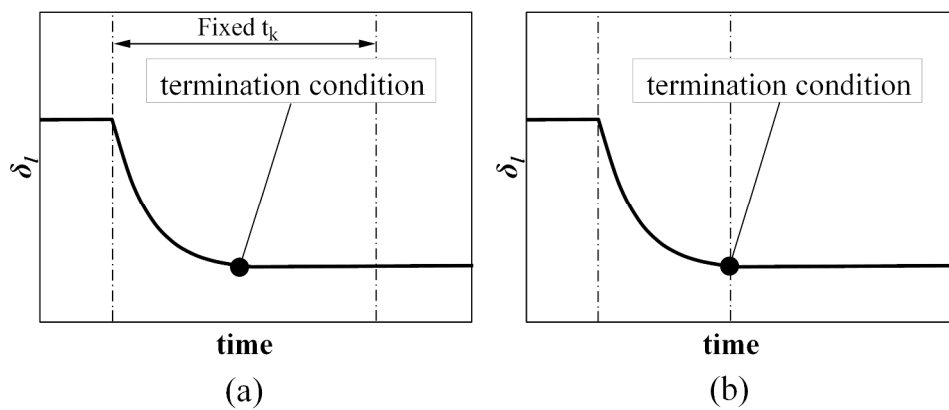


Figure 4. Deposit thickness reduction for fixed time (a) and condition-based (b) cleaning. The vertical lines indicate the start and end of the cleaning period.

250x106mm (300 x 300 DPI)

Accepted

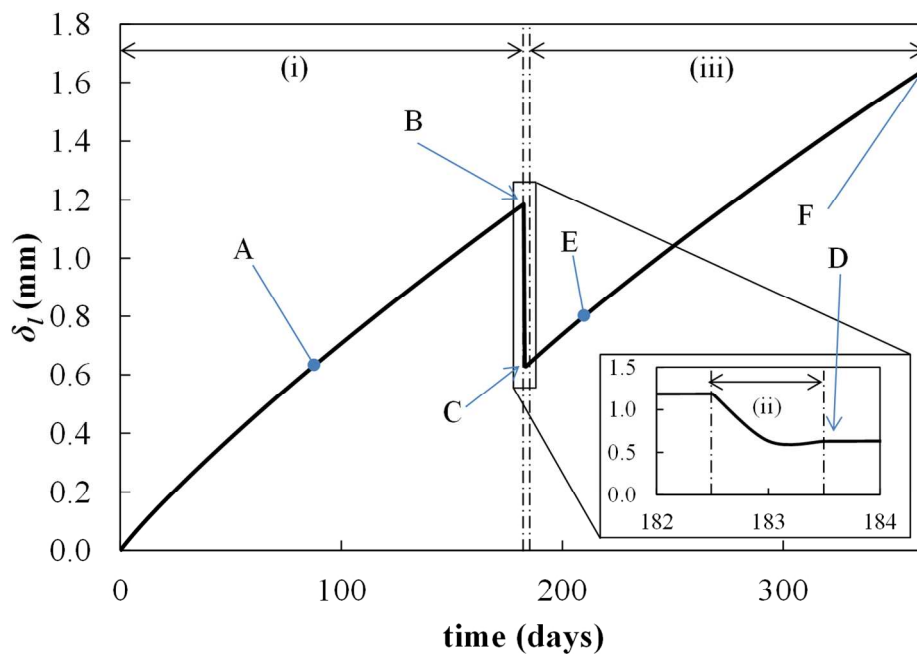


Figure 5. Deposit thickness at the midpoint of the tube ($z = 3.05\text{m}$) over time with a chemical cleaning after 6 months.
130x88mm (300 x 300 DPI)

Accept

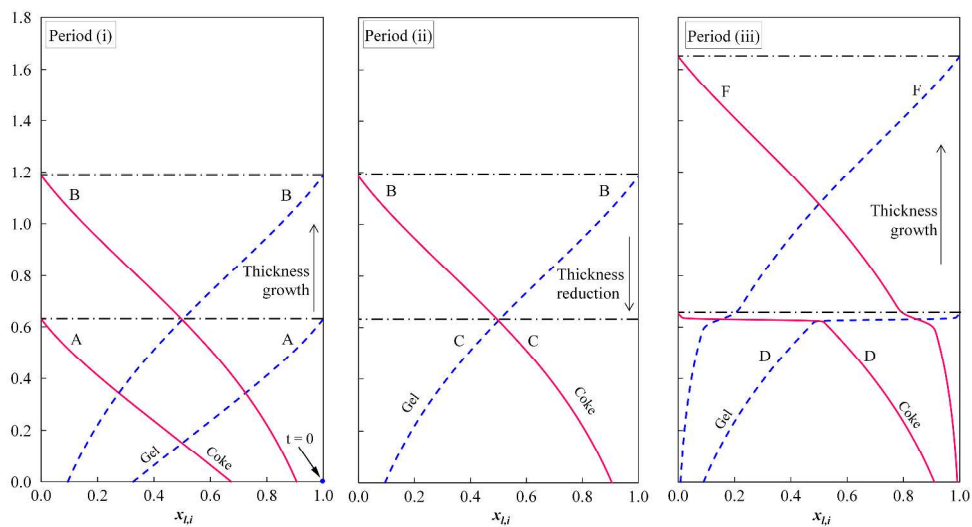


Figure 6. Thickness and radial (dimensional) concentration profiles at the tube midpoint ($z = 3.05\text{m}$), at key times in periods i, ii and iii (left to right).
569x312mm (300 x 300 DPI)

Accepted

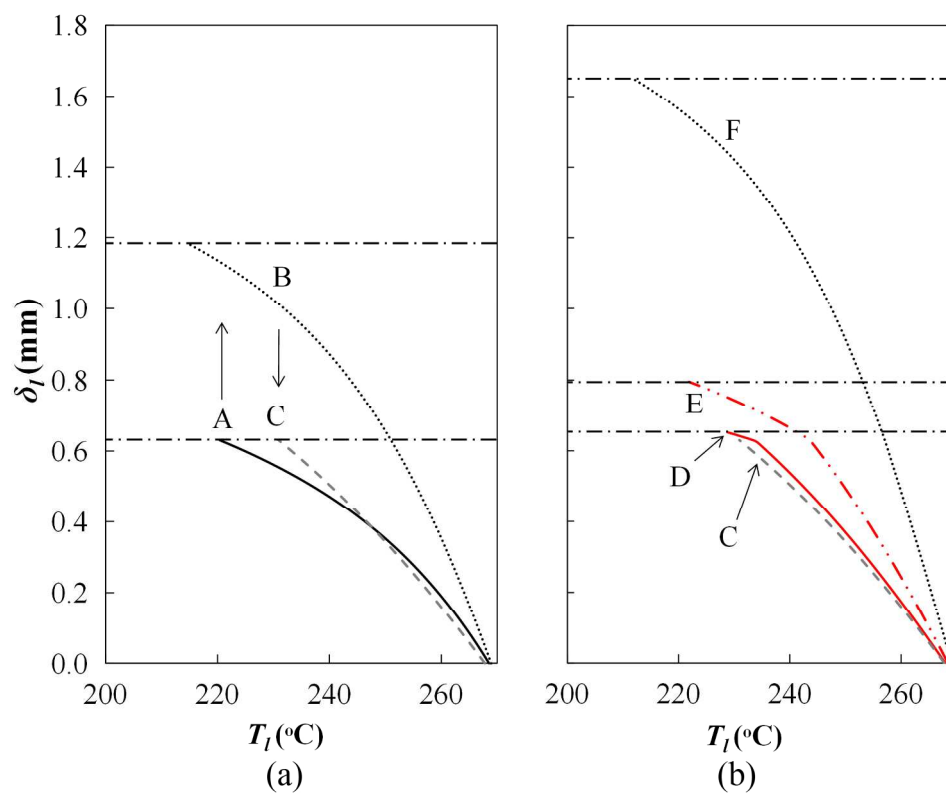


Figure 7. Fouling layer temperature profile at the tube midpoint ($z=3.05\text{m}$) at various times. 186x152mm (300 x 300 DPI)

Accepted

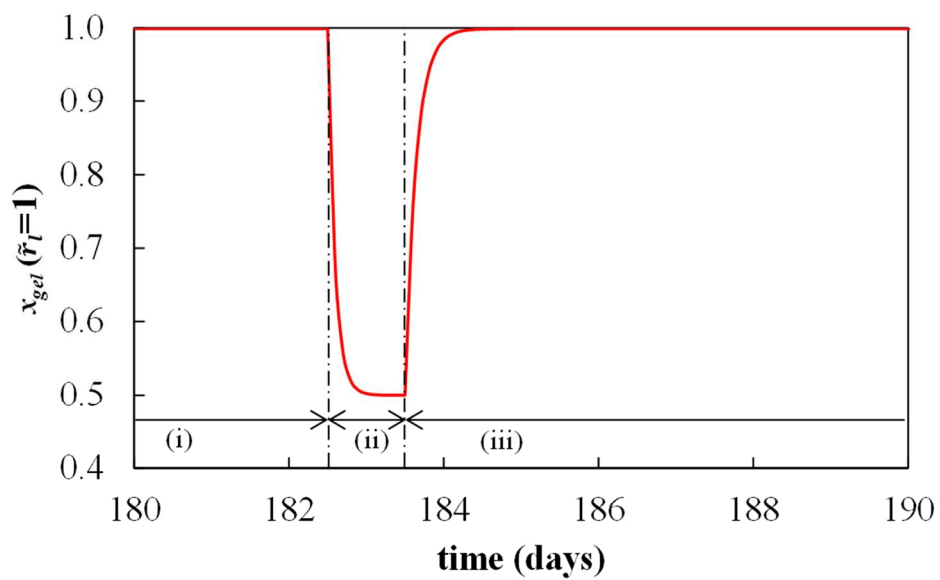


Figure 8. Volume fraction of gel at the deposit layer surface in the tube midpoint during periods i, ii and iii.
96x58mm (300 x 300 DPI)

Accepted

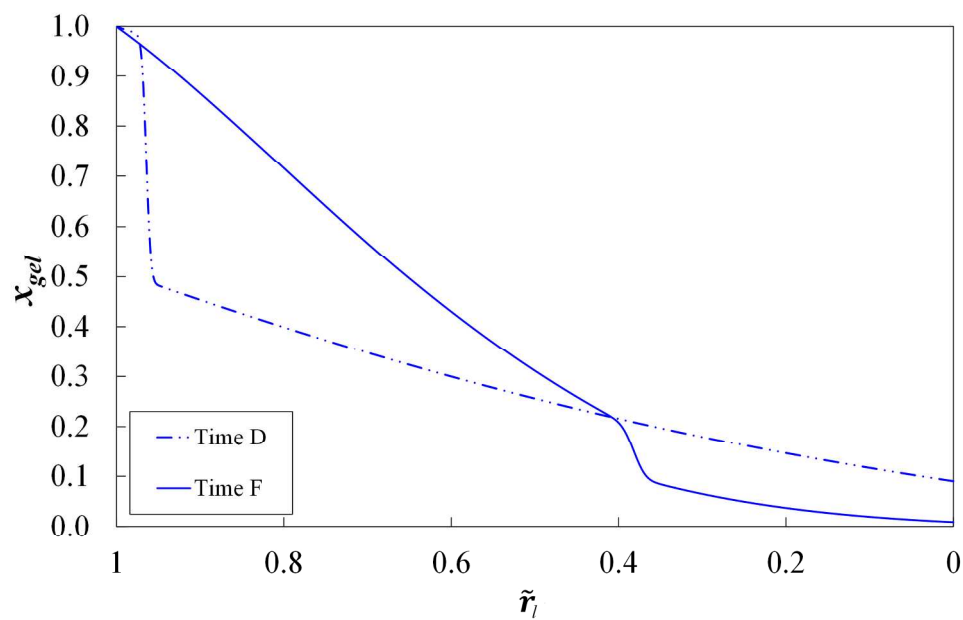


Figure 9. Gel fraction profiles against transformed radial coordinate, at the tube midpoint, at time D (just after resumption of fouling) and at time F (6 months later).
193x126mm (300 x 300 DPI)

Accepte

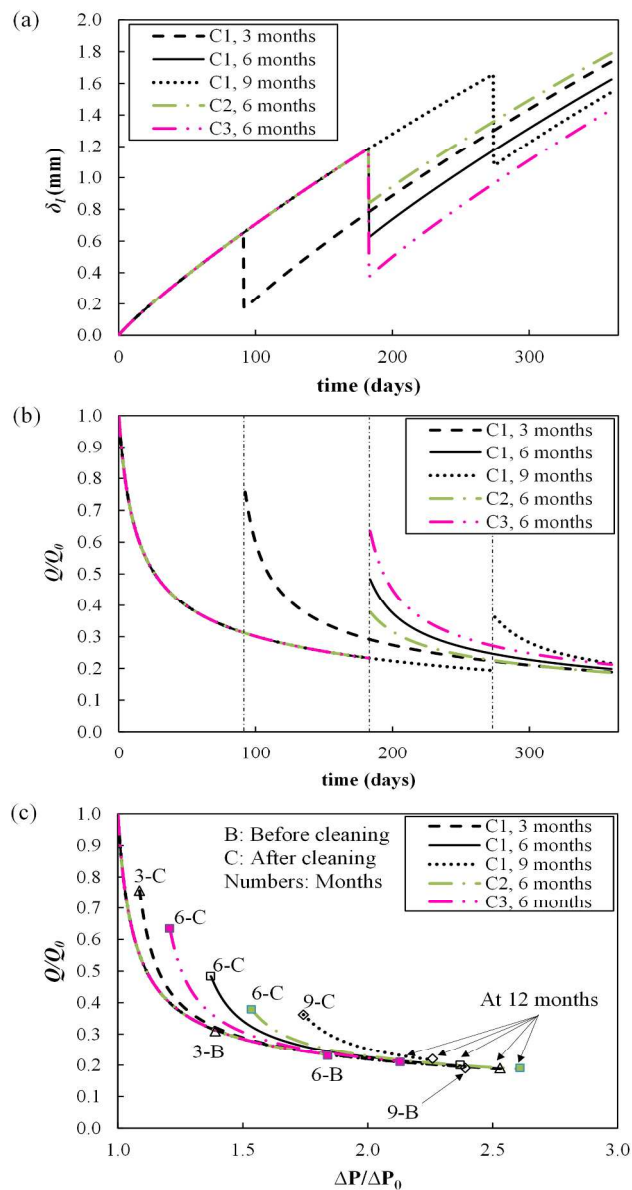


Figure 10. Deposit thickness at the tube midpoint ($z = 3.05\text{m}$) (a), Heat duty (normalized to clean duty) (b) and Thermo-hydraulic performance (c) for a single chemical cleaning C1 after 3, 6 and 9 months and cleanings C2, C3 after 6 months.
144x266mm (300 x 300 DPI)

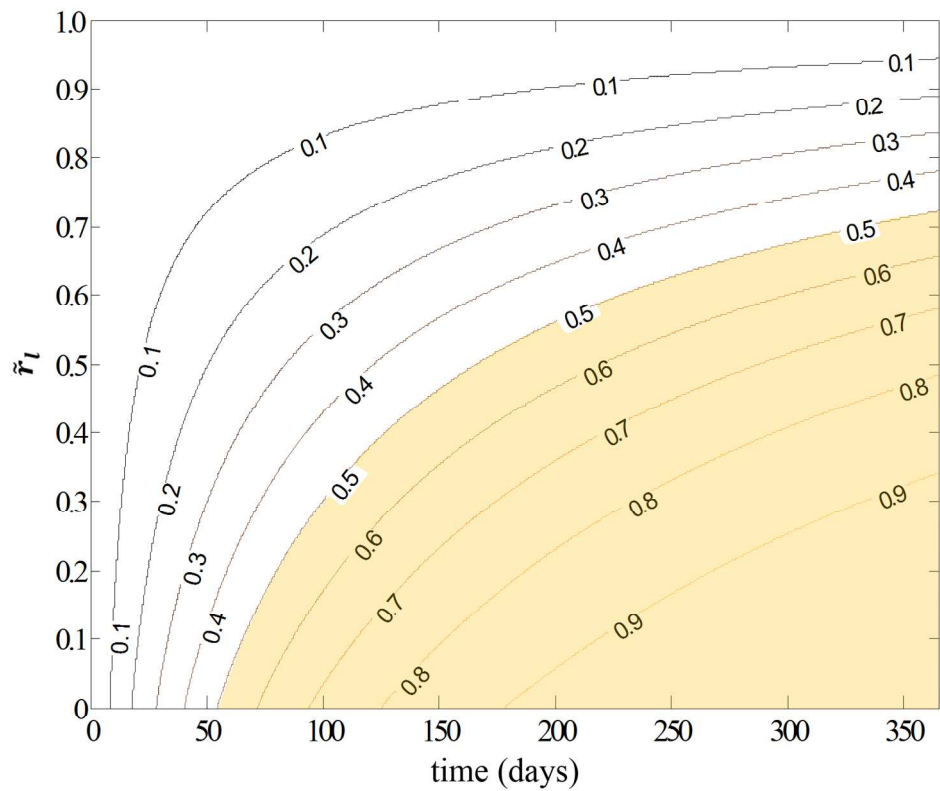


Figure 11. Volume fraction of coke as function of the radial coordinate (dimensionless) and time at the tube midpoint ($z = 3.05\text{m}$) for a year without cleaning. The shaded area indicates the non-removable portion by chemical cleaning C1.

150x123mm (300 x 300 DPI)

Accep

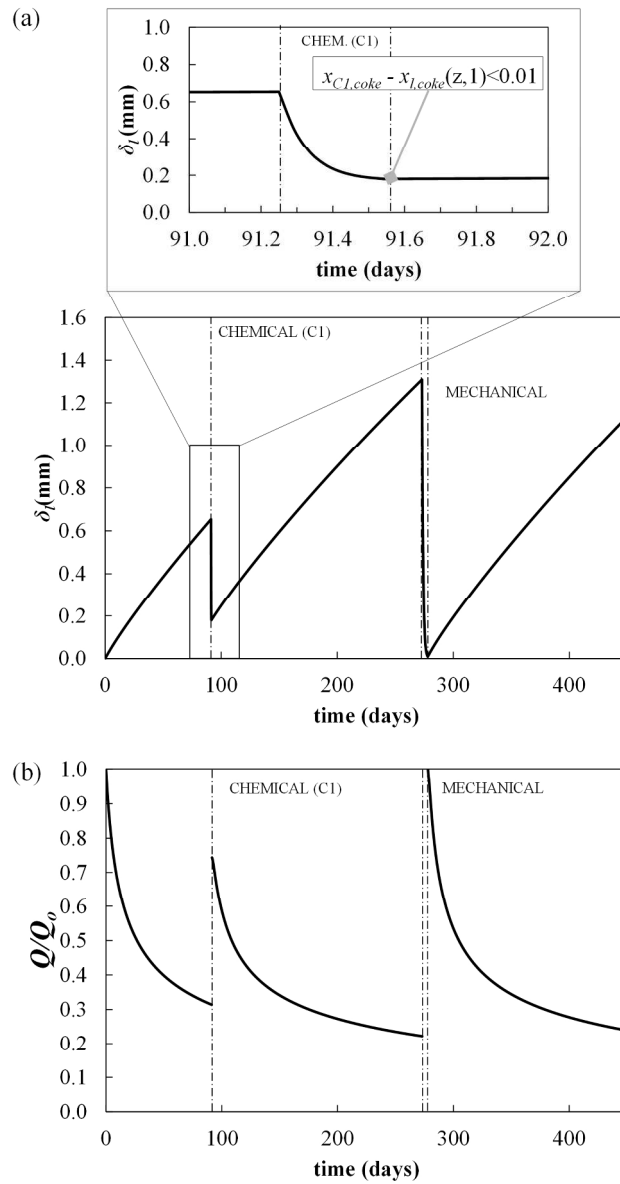


Figure 12. Deposit thickness at the tube midpoint ($z = 3.05\text{m}$) (a) and heat duty (b) over time for operation during 450 days with condition-based chemical (C1) and fixed-time mechanical cleanings.

134x246mm (300 x 300 DPI)

AIChE

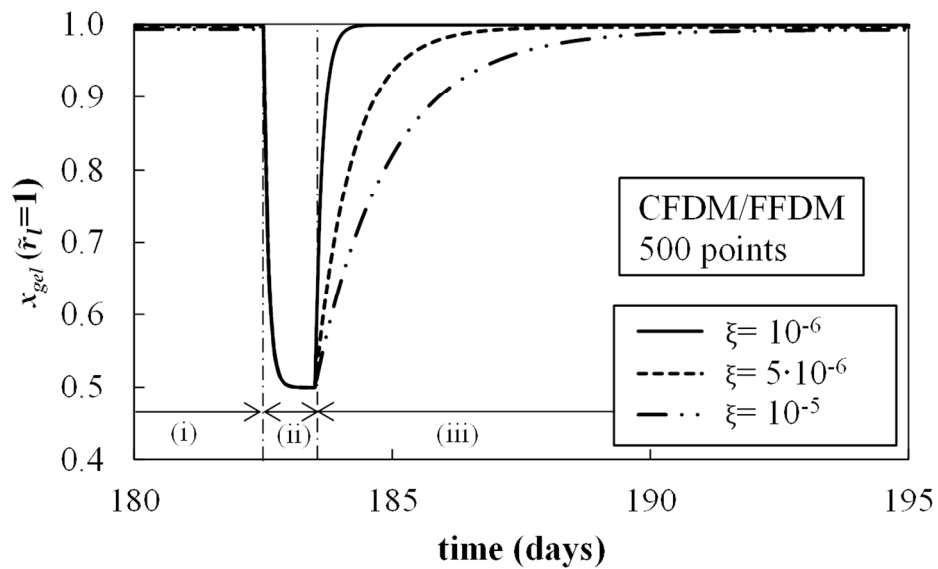


Figure 13. Effect of ξ on gel volume fraction at the surface of the layer during period (ii) and beginning of (iii) (re-start)
119x71mm (300 x 300 DPI)

Accepted

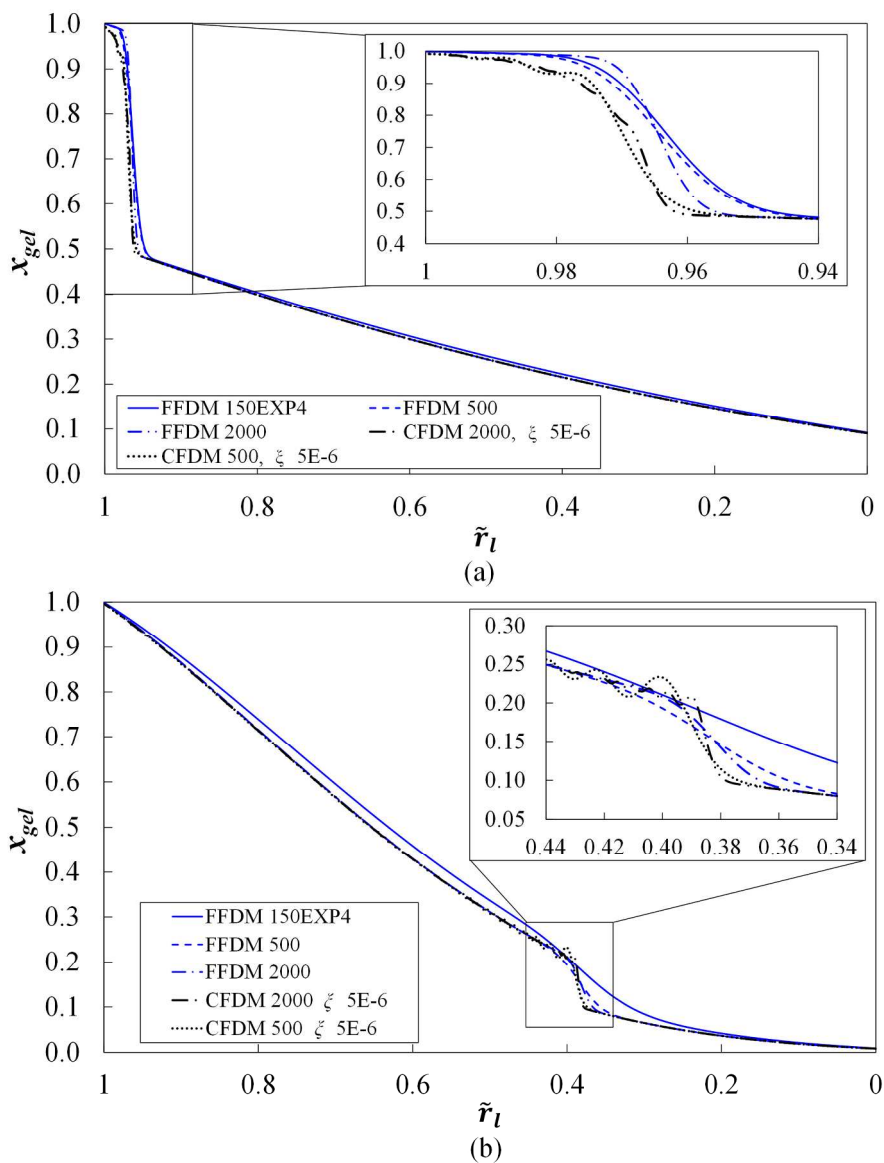


Figure 14. Gel fraction profiles against transformed radial coordinate for various discretization methods, at the tube midpoint, at time D just after resumption of fouling (a) and at time F, 180 days later (b).
186x241mm (300 x 300 DPI)

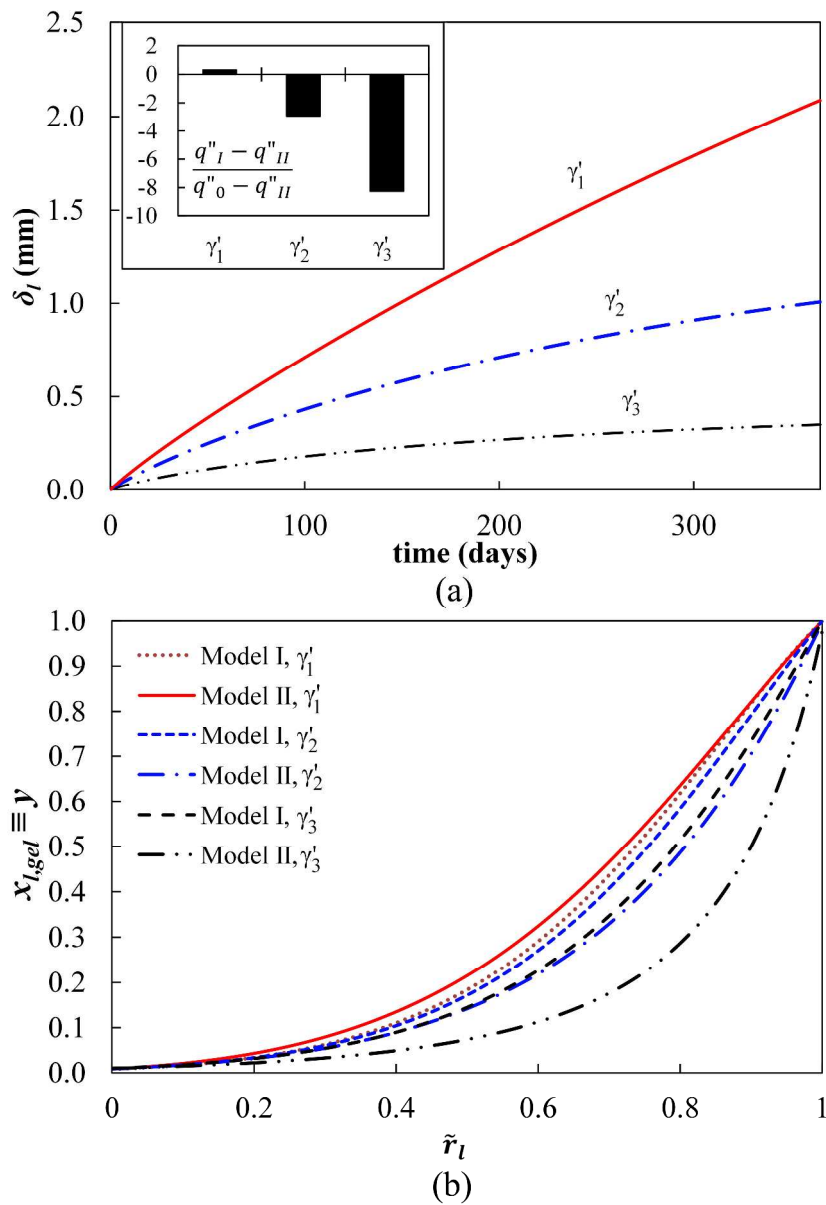


Figure 15. Comparison of models I and II for fouling build-up for 3 values of γ' over a year of operation at the tube midpoint ($z=3.05$): (a) deposit thickness and impact on heat flux (in the inside); (b) concentration radial profile after a year.
422x584mm (300 x 300 DPI)

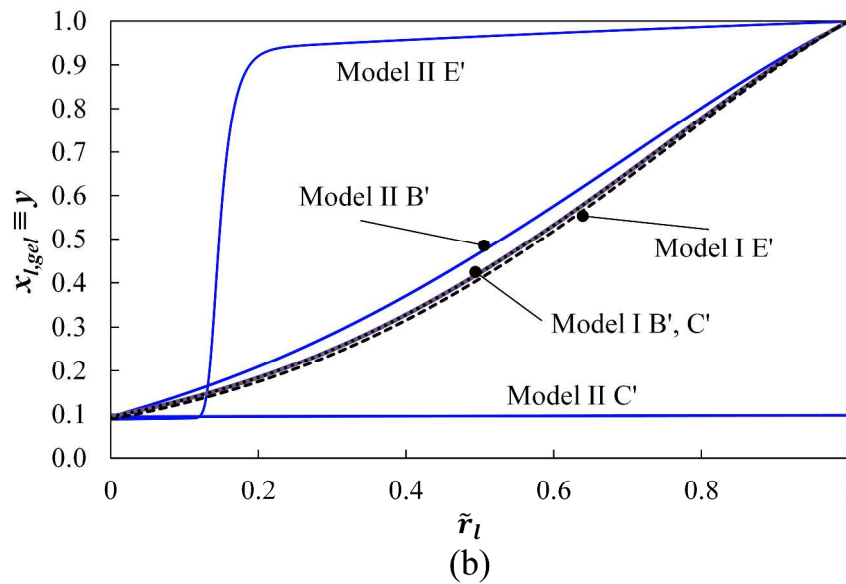
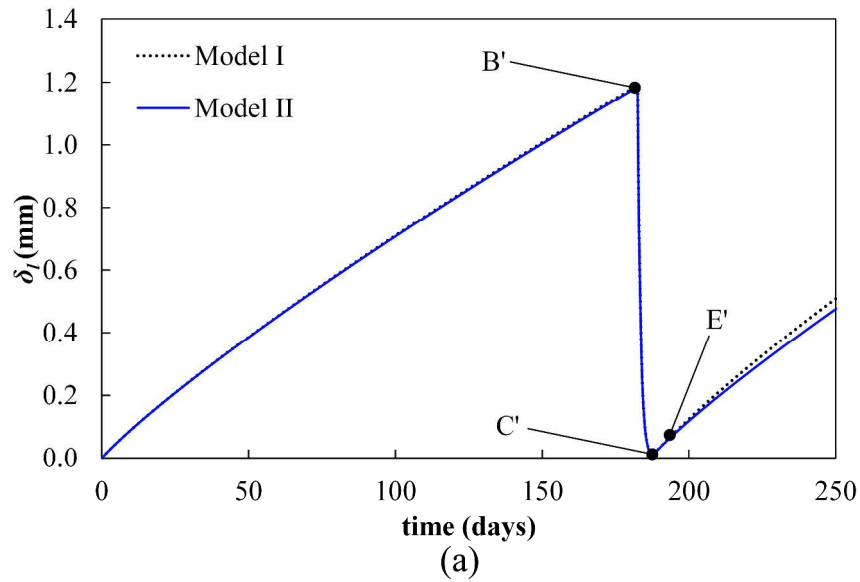


Figure 16. Comparison of models I and II at the tube midpoint ($z=3.05$) for fouling build up with mechanical cleaning after 6 months: (a) deposit thickness; (b) concentration radial profile at times B', C' and E'.
420x566mm (300 x 300 DPI)